Atmos. Chem. Phys. Discuss., 13, 379–435, 2013
www.atmos-chem-phys-discuss.net/13/379/2013/
doi:10.5194/acpd-13-379-2013

Atmospheric Chemistry and Physics Discussions

Long term changes in the upper stratospheric ozone at Syowa, Antarctica

K. Miyagawa[1], **I. Petropavlovskikh**[2], **R. D. Evans**[3], **C. Long**[4], **J. Wild**[4,5], **G. L. Manney**[6,7], **and W. H. Daffer**[8]

[1]Japan Meteorological Agency, Aerological Observatory, Tsukuba, Ibaraki, 305-0052, Japan
[2]Cooperative Institute for Research in Environmental Sciences, University of Colorado, Boulder Colorado, USA
[3]NOAA/OAR/ESRL Climate Monitoring Division, 325 Broadway, Boulder, Colorado, USA
[4]NOAA/NWS/NCEP/Climate Prediction Center, Silver Spring, USA
[5]NOAA/NWS/NCEP/Climate Prediction Center, Wyle ST&E, McLean, VA, USA
[6]NorthWest Research Associates, Socorro, NM, USA
[7]New Mexico Institute of Mining and Technology, Socorro, NM, USA
[8]Jet Propulsion Laboratory, California Institute of Technology, Pasadena, CA, USA

Received: 9 November 2012 – Accepted: 14 December 2012 – Published: 7 January 2013

Correspondence to: K. Miyagawa (koji.miyagawa@gmail.com),
I. Petropavlovskikh (irina.petro@noaa.gov)

Published by Copernicus Publications on behalf of the European Geosciences Union.

Abstract

Analyses of stratospheric ozone data determined from Dobson Umkehr measurements since 1977 at the Syowa (69.0° S, 39.6° E), Antarctica station show a significant decrease in ozone at altitudes higher than that of the 4 hPa pressure level during the 1980s and 1990s. Ozone values over Syowa have remained low since 2001. The time series of upper stratospheric ozone from the homogenized NOAA (/2) SBUV 8.6 overpass data (±4°, 24 h) are in qualitative agreement with Syowa station data. Ozone recovery during the austral spring over Syowa station appears to be slower than predicted by the Equivalent Effective Stratospheric Chlorine (EESC) curve. The long-term changes in station's equivalent latitude are derived from MERRA analysis at ∼2 hPa and ∼50 hPa. These data are used to attribute some of the upper and middle stratospheric ozone changes to the changes in vortex position relative to station location. In addition, high correlation of the Southern Hemisphere Annular Mode (SAM) with polar upper stratospheric ozone during years of maximum solar activity points toward a strong relationship between the strength of the Brewer-Dobson circulation and the polar stratospheric ozone recovery. We have analyzed the results of ozone profiles over Syowa determined from measurements of the Umkehr effect by Dobson ozone spectrophotometers. The ozone depletion attributable to CFCs is clearly visible in the record, but the recovery is slower than predicted. Further research indicates that dynamical and other chemical changes in the atmosphere are delaying the recovery over this station.

1 Introduction

The ozone hole was originally discovered by Farman et al. (1985) in the 1980s, and the depletion of ozone accelerated rapidly during the end of the 20th century (Solomon, 1999), with a leveling off of the annual depletion in the early part of the 21st century (Salby et al., 2011). Molina and Roland (1974) predicted depletion of the ozone

ACPD
13, 379–435, 2013

layer by photochemical reactions with man-made CFCs, which were transported to the stratosphere. In the middle and upper stratosphere (above about 25 km), ozone destruction occurs through the gas phase catalytic reaction with chlorine atoms and through photochemical destruction. Conversely, ozone depletion in the lower stratosphere (height of about 15–20 km) takes place through the heterogeneous reaction on the surface of polar stratospheric clouds (PSCs: Polar Stratospheric Clouds) (Solomon et al., 1986). PSCs contain particles of water vapor (H_2O), nitric acid (HNO_3), and sulfuric acid (H_2SO_4), created under the specific atmospheric condition of low temperature in the Polar lower stratosphere. The upper stratospheric ozone depletion at the Northern middle latitudes has shown signs of recovery beginning in 1997 as a result of the Montreal Protocol initiated control of CFCs (Newchurch et al., 2003). Although the first stage of ozone recovery, described as a slowdown of an ozone reduction, has been already observed, the second stage of the statistically significant ozone increase has not yet been reached (Solomon et al., 2005; WMO, 2011). Even at the current stage of enhanced control of CFC production, the balloon, satellite and ground-based ozone observations in the Antarctic region show high year-to-year variability in the ozone hole region, and reveal a delay in ozone recovery as compared to the mid-low latitude trends (WMO, 2011; and references therein). The Syowa ground-based station (69.0° S, 39.6° E) in Antarctica has been collecting ozone profiles from Dobson Umkehr measurements since 1977 (Miyagawa and Sasaki, 2009), providing information on long-term changes in the upper and middle stratosphere. The ozone variability in the upper stratosphere is primarily controlled by chemical reactions influenced by the anthropogenic ozone-depleting substances (ODS), as compared to the dynamically driven troposphere, and thus is expected to provide information for early detection of ozone recovery (Newchurch et al., 2003). However, continuous increase of greenhouse gases in the atmosphere and enhanced cooling of the stratosphere can affect recovery of the ozone layer (Waugh et al., 2009; Li et al., 2009; Oman et al., 2010 and references therein). While the ODS levels have been significantly decreasing after reaching a maximum in 1998, stratospheric temperature has been decreasing in re-

ACPD
13, 379–435, 2013

sponse to the increase in concentrations of greenhouse gas chemicals such as water vapor, CO_2 and methane. Cooling of the upper stratosphere reduces ozone loss rates (mainly through the $O + O_3 = 2O_2$ chemical cycle), and therefore results in faster ozone recovery (Rosenfield et al., 2002). Lower temperatures due to climate change in the polar lower stratosphere increase heterogeneous conversion of chlorine and bromine reservoir species to more active forms, leading to a decrease in ozone. In this paper we discuss the long-term trend of polar upper stratospheric ozone in relation to the ODS concentration changes over the Antarctica. The ODS concentrations are often represented by the time series of the EESC (equivalent effective stratospheric chlorine) concentration that are based on the known budgets of the anthropogenic and natural sources of CFCs, halogens and bromines, understanding of the life-time of these species in the atmosphere, and estimates of the transport/mixing of ODS from the tropical troposphere to stratosphere and from tropics to high latitudes by a meridional transport and vertical mixing (Brewer Dobson Circulation, or BDC). The ODS concentrations over Polar region (or EESC curves) are defined by the "age of the transported air" (WMO, 2011).

In addition to the chemical reaction mechanism, stratospheric ozone is radiatively coupled to atmospheric dynamics, and can be affected by meridional transport (BDC), or stratospheric temperature changes related to heat transport through wave activity and to variations in the polar vortex (Jiang et al., 2008; Hitchman and Rogal, 2010); ozone depletion has been shown to affect the strength of the polar vortex (Thompson and Solomon, 2002; Perlwitz et al., 2008; Fogt et al., 2009; Li et al., 2010; Oman et al., 2010; Son et al., 2010). While the SH has weaker planetary wave activity than the NH, the change in the BDC contributes strongly to ozone variability over the South Pole region. A relationship between the Antarctic stratospheric ozone depletion, strengthening of the polar circulation in the SH stratosphere and the Southern Annular Mode (SAM) index has been found in observations and discussed in many papers (Kushner et al., 2001; Thompson and Solomon, 2002, 2005; Arblaster and Meehl, 2006; Jiang et al., 2008; Fogt et al., 2009; Wang et al., 2011). The intra-annual ozone-SAM link has

ACPD
13, 379–435, 2013

also been identified in coupled chemistry-climate models (Perlwitz et al., 2008; Son et al., 2008; Fogt et al., 2009; Thompson et al., 2011). The largest variability in the Antarctic stratosphere associated with the SAM signal is observed in the September through December period. A positive trend in SAM is also related to a stronger planetary wave activity in stratosphere and prolonged westerly anomalies (Li et al., 2010). At the same time, Antarctic polar ozone long-term depletion has influenced the austral summer tropospheric circulation (SAM) in the Southern Hemisphere (Perlwitz et al., 2008). Correlation of the SAM index and Syowa ozone data interannual variability is addressed in this paper.

The El Nino Southern Oscillation (ENSO) (Diaz and Markgraf, 1992) is the largest climatic signal observed in many meteorological data sets, not just over the equator, but also in remote areas. ENSO is found to be responsible for the generation of a type of Rossby wave that travels from the Equator towards the Poles, and is responsible for coupling between the stratosphere and troposphere over Antarctica (Hoskins and Karoly, 1981; Randel, 1987, 1988; Perlwitz and Harnik, 2004; Turner, 1994; Hu and Fu, 2009; Ialongo et al., 2011). The ENSO signal at sea level pressure and at high latitudes is amplified when it is in phase with SAM (Fogt and Bromwich, 2006), for example, during the 1990s. The ENSO signal for the time period between 1958 and 2001 is highly anti-correlated with SAM at the surface, but has weaker correlation (negative) at 50 and 30 hPa atmospheric levels (Haigh and Roscoe, 2006). It shows high correlation during austral summer, when 25 % of the SAM inter-annual variability is linearly related to ENSO (L'Heureux et al., 2006). Therefore, the relationship between ozone variability and ENSO or SAM signal is highly non-linear, where the SAM's decadal changes enable shifts in climate regimes (Yuan and Yonekura, 2011). The change in sea level pressure affects the westerlies, which therefore create a stronger polar vortex, and thus affect polar ozone (Hu and Fu, 2009).

The impact of the 11-yr solar cycle and the stratospheric equatorial Quasi-Biennial Oscillation (QBO) on the Southern Annular Mode (SAM) in late winter/spring is discussed in the paper by Kuroda and Yamazaki (2010). Under an Easterly QBO mode,

ACPD
13, 379–435, 2013

the critical latitude shifts more toward the Pole, and planetary waves propagate to the stratosphere, which strengthens residual BDC and reduces ozone in the lower stratosphere. Similar results are also found by Haigh and Roscoe (2006), when SAM variability is analyzed in relation to the compound of solar and QBO signals as compared to using these signals separately. Moreover, significant stratospheric warming over the high latitudes in the Southern Hemisphere has been derived from Microwave Sounding Unit observations (Hu and Fu, 2009). Warming trends are related to the increases of the stratospheric eddy-heat fluxes during austral late summer and fall, which are caused by the increase of the wave propagation into stratosphere and adiabatic heating. Hu and Fu (2009) found close correlation with Sea-Surface Temperatures, which are influenced by the anthropogenic increase in the green-house gases. Future stratospheric warming will likely influence ozone recovery in the upper stratosphere (Waugh et al., 2009; Stolarski et al., 2010). Moreover, analysis of the coupling between stratospheric ozone variability and climate changes that are affecting dynamics and meteorology of the atmosphere and oceans in the Southern Hemisphere are of great importance for future ozone level predictions.

Since both QBO and ENSO influence polar stratospheric temperatures and wave activity (Hamilton, 1998), and therefore ozone, it is difficult to separate the signals. Using an equatorial zonal wind data archive for the 1958–2008 periods, Taguchi (2010) found ENSO-related changes in the phase and amplitude of the QBO signal that are related to the wave activity at the Equatorial region. However, there are modeling studies that find stratospheric polar temperature changes between El Nino (EN) and La Nina (LN) periods even when no QBO signal is included in the model (Sassi et al., 2004; Garcia-Herrera et al., 2006; L'Heuraux and Thompson, 2006). Clear differences in general circulation and total ozone distribution in the Southern Hemisphere are found between LN and EN years (Garfinkel and Hartmann, 2007; Hitchman and Rogal, 2010). Hitchman and Rogal (2010) showed that in months of August-September-October there is a strong relation between UTLS anticyclone near the tip of South Africa (SA), wave activity, and reduction of ozone distribution that is driven by ENSO events. Syowa sta-

ACPD
13, 379–435, 2013

tion is located along the longitude that intersects the location of the South African High anticyclone, and therefore is affected by the variability in regional meridional circulation and by ENSO variability, i.e. strong anticyclone forms near SA during EN phase, and stronger transport of ozone-poor air-masses to high latitude stratosphere occurs, thus affecting year-to year variability in stratospheric ozone over Syowa station.

Global warming (climate change) also affects stratospheric ozone layer depletion through sensitivity of the chemical reactions to the atmospheric temperature change. When the concentration of greenhouse gases increases in the atmosphere, the temperature of the troposphere rises (greenhouse effect) (Turner et al., 2006). At the same time more of the outgoing Earth infrared radiation becomes trapped in the troposphere instead of reaching the stratosphere. Therefore, this missing IR radiation does not balance out stratospheric cooling due to emission from the increase in stratospheric water vapor and carbon dioxide gases. The change of the heat balance reduces temperature in the stratosphere (Shindell, 2001). This effect is especially large in the polar lower stratosphere, and it strengthens the occurrence of the PSCs in winter. Therefore, it strengthens the Antarctic ozone-hole chemistry. Chemical processes on the surface of the PSC clouds release active chlorine and create conditions for rapid ozone destruction in both Antarctic and the Arctic region when the sun returns (Solomon et al., 1986; Solomon, 1999). Conversely, the temperature decline of the upper stratosphere leads to the increase in ozone (O_3), via an increase in the rate of the binding reaction of an oxygen molecule (O_2) and an oxygen atom (O). On the other hand, water vapor in stratosphere converts to hydrogen oxide (OH) molecules that destroy ozone, while OH also reacts with CFCs that create Chlorine compounds that also destroy ozone. Additionally, a change in the transport pattern known as the BDC tends to increase water vapor in the stratosphere, which also affects ozone layer (Garcia and Randel, 2008). It is important to distinguish the influence that climate change has on ozone layer depletion from the effects of ODS. While stratospheric ozone concentrations will recover with the reduction in ODS the impact of the stratospheric ozone change on the temperature

ACPD
13, 379–435, 2013

trend will be altered by the effects of the increase in the greenhouse gases (Stolarski et al., 2010).

Continuous monitoring by high quality ground-based observations is very important for detecting long-term changes in the ozone global distribution. The mechanisms that affect ozone on different time scales need to be investigated. The Dobson ozone spectrophotometer measurements provide not only estimates of total ozone column above the surface, but also vertical profile information. The Umkehr technique has been used since the 1930s (Götz et al., 1934) to derive the vertical ozone profile from zenith sky measurements. The algorithm is described elsewhere (Petropavlovskikh et al., 2009). The re-evaluated Umkehr datasets from the Syowa Japanese ground-based Dobson station (Miyagawa et al., 2009) are used for this study (Sect. 2). A further data refinement is described below.

The paper by Miyagawa and Sasaki (2009) describes trends determined in the austral spring-summer season from ozone profiles measurements at Syowa station using techniques similar to Reinsel et al. (2002). In this paper we are using the same data set (plus 4 more years), similar statistical methods, and investigate the contributions from other atmospheric parameters (Sect. 3). We compare the ozone trend derived from Umkehr measurements at Syowa station with the trend derived from the homogenized Solar Backscatter UV (SBUV) instrument satellite data that is restricted to the station over-pass (see details in Sect. 3.4). We investigate ozone trends in the upper stratosphere with respect to changes in temperature while also accounting for the changes in ODS. Moreover, we find that long-term changes in ozone at high latitudes and in the upper stratosphere cannot be fully explained by the ODS related chemistry. Therefore we include additional explanatory parameters in the statistical model and study their correlation with the long-term changes in the Umkehr ozone profile record over Syowa

Discussion Paper | Discussion Paper | Discussion Paper | Discussion Paper |

ACPD

13, 379–435, 2013

Long term changes in the upper stratospheric ozone at Syowa, Antarctica

K. Miyagawa et al.

2 Ozone data sets

Umkehr ozone profile measurements at Antarctic station Syowa (69.0° S, 39.6° E) are typically possible from late August to April. About 1508 data records were acquired by the Japanese Antarctic Research Expedition at Syowa Station between 1977 and 2011. The total number of usable ozone profiles derived from the observations of the Umkehr effect at Syowa is 928 in August–December and 580 in January–April. The fully automated system of Dobson Umkehr measurements was introduced for more frequent and higher quality data in 1994 (Miyagawa, 1996). All Umkehr data from Syowa station are available from the World Meteorological Organization (WMO) Ozone and Ultraviolet Data Centre in Toronto, Canada (WOUDC).

The limited data taken by Dobson instruments at Halley (73.5° S, 26.7° W), and Faraday (65.3° S, 64.3° W) stations in the Antarctic region from 1957 to 1972 are also investigated and compared to the Syowa record. The data at Halley station was acquired during the months of October (13 observations), February and March (7 observations). In addition, 40 Umkehr ozone profiles obtained at King Baudouin and 65 profiles at Faraday stations are used for the discussion of seasonal variability of stratospheric ozone prior to the ozone hole and to check the consistency with the early part of Syowa record.

In our study, we used vertical profiles of ozone derived from the measurements by the SBUV instruments on NASA's Nimbus-7 satellite and SBUV/2 instruments on NOAA-9, -11, -16, -17 and -18 satellites. The data record begins in October 1978 and is nearly continuous until the present. The data set is processed with the SBUV V8.6 algorithm (http://acd-ext.gsfc.nasa.gov/Data_services/merged/sbuv.alg_cal.html), and is provided by NOAA (C. Long, private communications in 2012).

ACPD
13, 379–435, 2013

3 Trend evaluation

3.1 Uncertainty for ozone profile retrieval

Umkehr observations have been routinely conducted at the Syowa Antarctic station for more than 30 yr. However, the Umkehr record at Japanese stations has evident discontinuities. The majority of the discontinuities are associated with the regular exchange of station instruments (instruments are replaced every 2 yr), which involves application of new calibration parameters (for total ozone measurements) and accounting for instrument-specific optical characteristics. The systematic errors are evaluated by simultaneous intercomparisons of each instrument (Dobson #119 and Dobson #122) with the reference instrument (Dobson #116). Through the reevaluation of Syowa's record as described in detail by Miyagawa and Sasaki (2009), most discontinuities in station's Umkehr time series are successfully corrected.

During the development of the UMK04 ozone profile retrieval algorithm (Petropavlovskikh et al., 2005), the a priori ozone data were based on an earlier version of ozone climatology (personal contact with G. Labow in 1999) and later published by McPeters et al. (2007). The climatology available in 2004 was based on 1982–2000 SAGE II (Stratospheric Aerosol and Gas Experiment) record and ozone sonde data that had inconsistent coverage at high latitudes. Therefore, for high latitude Umkehr retrievals (relevant for only the few stations that take Umkehr measurements at latitudes poleward of 60° S), the UMK04 algorithm uses the middle-latitude (50–60° S) a priori. For the analyses published in this paper, the Syowa data are processed by the UMK04 algorithm modified to include an updated a priori for 60–70° S. The updated a priori is based on the MLS 2007 climatology (McPeters et al., 2007), which at high latitudes relies on MLS (Microwave Limb Sounder) ozone profiles recorded aboard the UARS (Upper Atmosphere Research Satellite) satellite operated by NASA between 1991 and 2005 (Livesey et al., 2003).

Umkehr measurements at Syowa are affected by the elevation of the sun, which has seasonal dependence. This means that the range of SZA available for Umkehr profile

ACPD
13, 379–435, 2013

Long term changes in the upper stratospheric ozone at Syowa, Antarctica

K. Miyagawa et al.

retrievals changes rapidly during early spring and late fall. Typically, the UMK04 ozone profile retrieval algorithm normalizes the Umkehr measurements to 70-degrees SZA observation. In early spring and autumn, since the solar elevation is lower, it changes normalization to the observation at 80-degrees SZA. Change in the range of SZAs available for Umkehr retrieval creates a small, but significant bias in the UMK04 retrieved ozone profile. What could be even more detrimental for trend analysis, Umkehr measurements in 1988 and 1989 were taken only up to 80-degrees SZA. Therefore, temporal change in normalization of measurements can create a step change in the ozone time series. Therefore, in this study we apply the UMK04 retrieval algorithm to all records uniformly normalized to 80-degrees SZA.

3.2 Statistical trend model

Strong inter-annual and seasonal variability in stratospheric ozone over Syowa requires statistical models to attribute long-term changes to natural and anthropogenic sources (WMO 2011 and references therein). Besides the commonly used regressions against the Solar cycle and QBO phase, including the analysis of the residuals to determine statistical significance of derived trends (Reinsel et al., 2002; Newchurch et al., 2003), dynamical proxy terms were also used in previous studies of ozone data (Steinbrecht et al., 1998; Appenzeller et al., 2000; Weiss et al., 2001; Reinsel et al., 2005; Zanis et al., 2006; Dhomse et al., 2006; Wohltmann et al., 2007; Vyushin et al., 2007; Krzyścin et al., 2009) including so-called Equivalent Latitude (EqLat, the latitude that encloses the same area poleward of it as a given potential vorticity contour, Butchart and Remsberg, 1986) of the stations that accounts for meridional transport and thus represents a dynamical proxy (Butchart and Remsberg, 1986; Schoeberl et al., 1992; Manney et al., 1994, 1999; Lu et al., 2009, 2011; Nash et al., 1996; Pan et al., 2011). However, the studies mentioned above addressed ozone variability observed mostly in the Northern Hemisphere. In this paper we include several dynamical proxies in the statistical regression model, such as SAM, ENSO, Heat flux (55–75° S average at 10 hPa), and Equivalent latitude that help to capture the inter-annual ozone variability

Discussion Paper | Discussion Paper | Discussion Paper | Discussion Paper |

ACPD

13, 379–435, 2013

Long term changes in the upper stratospheric ozone at Syowa, Antarctica

K. Miyagawa et al.

observed in the upper and middle stratosphere over Syowa station. The attribution of ozone variability described in this paper is specific to the processes affecting ozone at the Antarctic coastal area, and can be different for other geo-locations above the Antarctic continent because the polar vortex exhibits non-zonal features during the austral spring time (Hassler et al., 2011).

The accuracy of the ozone trend analysis depends on the successful removal of natural variability from the ozone record. The statistical trend model used in this paper is defined as the 1st order auto regression (AR(1)) fit in the data with seasonal cycle, effects of solar activity (SOR), QBO, SAM, ENSO, Heat flux, and EqLat of the station. The statistical model fit provides attributions of the above parameters to the Syowa ozone record and reduces variability in residual data prior to assessing how remaining long-term changes are related to the anthropogenic forcing (WMO, 1992). The “broken stick” model (Reinsel et al., 2002, 2005) is used to analyze data for linear changes before and after a chosen “turning point”, which is a date that is associated with the reverse in the annual growth rate of the atmospheric ODS concentrations. The model is set to detect a change in the linear trend after the “turning point” and to estimate statistical significance in this change by using the CUSUM method (Reinsel et al., 2002; Newchurch et al., 2003). Another approach is to use the EESC curve as one explanatory parameter and assess changes in the data that agree or disagree with prescribed rate of increase and reduction of the ODS concentrations in the atmosphere (Zanis et al., 2006). Equation (1) describes the multiple regression model, which consists of linear terms (linear trend and change in trend) and/or several proxies that account for the anthropogenic and natural variability of ozone as described above (Reinsel et al., 2002, 2005; Yoshimatsu et al., 2005).

$$[Y]_t = a_0 + a_1[X_1]_{t-\mathrm{d}t_1} + a_2[X_2]_{t-\mathrm{d}t_2} + \ldots + a_m[X_m]_{t-\mathrm{d}t_m} + e_t \tag{1}$$

Here,X_m is the explanatory parameter, a_0 is an intercept and a_m is a partial regression coefficient, and e_t is the unexplained noise term assumed to be autoregressive with

ACPD
13, 379–435, 2013

time lag of 1 month. t is a number of months from January 1979, and dt is the optimum lag value of the proxy.

Proxy datasets

The following datasets are used as proxies (Table 1). The solar activity (SOR) index is represented by the solar flux (3,750 MHz) observed by National Astronomical Observatory of Japan. For QBO proxy we use the east-and-west zonal wind at 50 hPa and 30 hPa over Singapore (1° N/104° E) (Freie Universität Berlin Physics of the Middle Atmosphere). In addition, we apply the SAM index based on the UK Met database (Marshall, 2003). The NOAA Climate Prediction Center (CPC) (private communications with C. Long, in 2010) stratospheric analysis data are used as the proxy for the upper stratospheric temperature changes over Syowa (Finger et al., 1993; Gelman, 1991).

The El Niño Southern Oscillations (ENSO) index is taken from the NOAA/NCEP analysis. The Heat Flux is the parameter that represents correlation of the meridional temperatures and winds. Under strong wave activity the Heat Flux increases. It is calculated as divergence in stationary waves 1–3 (the strongest wave numbers) and is taken as an average between 45° and 75° S. This information is obtained from the NASA MERRA reanalysis. The Modern Era Retrospective-analysis for Research and Applications (MERRA) is available online through the Modeling and Assimilation Data and Information Services Center (MDISC). Data provided are daily averages since 1979. Since the heat flux is highly variable parameter, only days that are co-incident with Umkehr measurements are used in monthly averages.

Figure 1 shows time series of ozone monthly averages (a) and all proxies used in the trend model fit, such as QBO (b), ENSO (c), Solar (d), SAM (e), EqLat (f), Heat flux (g) and Aerosol optical depth (h). Heat flux uses 10-hPa of 45–75° S, and EqLat is used at 1300 K. Aerosol optical depth (AOD) is defined as monthly averages over 40–45° N to detect the events of volcanic eruption.

The correlation coefficient (R) and root mean square deviation (RMSD) of the residual is provided in Table 2 and represents the quality of the fit. Sequential addition of

ACPD
13, 379–435, 2013

proxies to the regression model and assessment of changes in R (or RMSD) of residuals allows for evaluation of independency of the chosen proxies for trend analysis. Correlation analysis of variability in different proxies also helps to eliminate non-orthogonal terms from the model (see Table 2).

In order to optimize the autoregressive model that fits the observed ozone variability, the time lag has to be determined for all explanatory variable time series. Results are shown in Table 2 (Sect. 2). For example, the application of the lag to the Singapore winds (QBO) time series has been applied in many studies of ozone trends (Zerefos et al., 1992). The lag represents the time it takes for the transport to affect ozone at higher latitudes. A significant influence of volcanic eruption on total ozone was found in the northern latitudes (Mäder et al., 2007). The application of the northern-latitude AOD time-series for analysis of data collected in the Polar southern latitudes requires application of the time-lag. Poberaj et al. (2011) suggest that ozone depletion due to chemical reactions on volcanic aerosol surfaces was compensated by the QBO and EP-flux enhanced BDC transport, such that the effect of Pinatubo eruption was not observed in Southern Hemisphere until 1992 (Poberaj et al., 2011) (See results in Table 2, part 2). The lag of 18 months in the ENSO record is determined for ozone variability in layer 8 of Syowa data. Garfinkel and Hartmann (2007) have discussed ENSO and QBO interferences and their effects on the temperature in Polar stratosphere. They found the typical lag of ENSO in the temperature record at 10 hPa and poleward of 70° S was one month or less, which was related to the anomalous heat conversion caused by the wave breaking in the stratosphere, and where the radiation relaxation happens more quickly than at 50 hPa level (Newman et al., 2001). This finding is likely to be similar to the upper stratospheric ozone record through the strong temperature/ozone chemistry relation. They also found an auto-correlation in the 10 hPa temperature record at a 12 month lag. This suggests that the Antarctic vortex has some “memory” for the ENSO signal that could last for at least one year. ERA-40 analysis temperatures at 10 hPa were used in this study, and the authors noted that the 12 month lag could be an artifact of the ERA-40 data assimilation.

ACPD
13, 379–435, 2013

A similar lag was discussed by Zerefos et al. (1992), who found a 43 month long wave in the spectral analysis of the total ozone time series. The authors could not explain it by any physical processes. Possible mechanisms for a lag as long as 18 months for ENSO need to be investigated further. Heat flux and SAM were found to have 16 and 2 month time lags, respectively, for layer 8 (4–2 hPa). It is important to note here that the derived time lag is also altitude dependent, corresponding to different processes governing the upper, middle and lower stratosphere.

After removing inter-annual variability in ozone data associated with the above parameters, we address the remaining long-term changes in ozone and the relationship to changes in ODS.

3.3 EESC trend curves

The EESC (Equivalent Effective Stratospheric Chlorine) time series are used to explain ozone depletion or recovery rates that are associated with changes in the ODS concentrations in the atmosphere (Douglass et al., 2006; Newman et al., 2006; WMO, 2007, 2011; Oman et al., 2010). The Polar EESC curves have been produced with settings that correspond to different assumptions regarding the mean age of air (how long it takes to transport the air with ODS chemicals from surface to stratosphere in tropics, and then from tropics to high latitudes) and by assuming the number of years (typically half of the age) to define the width of the air spectrum that depends on the life time of the ODS chemicals and transport pathways that change with the altitude and latitude of the observations. The effective chlorine includes all chlorine and bromine atoms of halogen species that destroy ozone. The contribution of bromine species is enhanced by Alfa coefficient that represents the greater efficiency of bromine (10 times for this case) in ozone destruction as compared to chlorine species (WMO, 2011). Three sets of EESC time series are used in analysis of the ozone records. The EESC curves are generated by the Goddard auto-mailer (http://acdb-ext.gsfc.nasa.gov/Data_services/automailer/index.html). Figure 2 shows the time series of three sets of EESC curve after normalization to zero level at the beginning of 1979. The first set (black line in

Figure 2) is chosen to represent EESC concentrations for the middle latitude upper stratosphere. It is based on the choice of 4 yr for age of air, 2 yr for air spectrum width distribution, and the 2010 WMO scenario for the ODS fractional release rates (Newman et al., 2007; Oman et al., 2009). However, the mean age of air varies with altitude and latitude (Waugh and Hall, 2002) and changes over time (Douglass et al., 2008; Waugh, 2009).

We chose two additional EESC sets generated by the NASA Goddard auto-mailer to represent the effective chlorine levels for the South Polar stratosphere. The first curve (Polar 2) is based on 5.5 yr of age of air and reaches its maximum in 2001. The second polar curve (Polar 3) exhibits maximum in 2008. It is modeled using 10 yr to define the mean age of air at upper stratospheric levels at high latitudes. This number is based on the MIPAS (Michelson Interferometer for Passive Atmospheric Sounding) measurements of SF_6 that Stiller et al. (2008) used to determine time for tropospheric air masses to be transported to the stratosphere and across the latitudes. These authors presented the zonally averaged SF_6 data taken aboard the Envisat satellite in 2002–2004 as a function of altitude and latitude. The analysis of 2002–2004 periods of MIPAS satellite measurements of the SF_6 and CO_2 suggests that the average mean age of air for polar stratosphere is about 10 yr. However, the authors also noticed high interannual and seasonal variability in the age of air, which they suggest is related to mesospheric intrusions of SF_6 depleted air into polar stratosphere at the end of the winter season.

3.4 Comparison of Umkehr data with SBUV (/2) satellites data

Long-term upper stratospheric ozone observed by the series of the SBUV (/2) satellites data is compared with Umkehr ozone measurements taken over the Syowa station. The satellite ozone data are retrieved using V8.6 (DeLand et al., 2012; Bhartia et al., 2012; McPeters et al., 2012). V8.6 data differ from V8 by the use of different ozone climatology, absorption cross section, OMI-based cloud height climatology and internal cross calibration technique without external adjustment (DeLand et al., 2012).

ACPD
13, 379–435, 2013

Currently, there are several sets of the SBUV V8.6 data that are available as individual unadjusted satellite records that periodically overlap, as zonally averaged and merged ozone data time series (http://acd-ext.gsfc.nasa.gov/Data_services/merged/) or as statistically adjusted cohesive SBUV time series (private communication with C. Long of NOAA/NWS). In order to carry the most relevant comparisons with ground-based data, satellite data are selected for Syowa station over-pass conditions, which limit data for time co-incidence within 24-h of Umkehr measurements and for location within the 4 by 4° box centered at the geophysical location of Syowa station. We compared a long-term ozone variability derived from version 8 (V8.0) and version 8.6 (V8.6) data against Umkehr data at Syowa station. In this paper we present results from V8.6 MOD (Merged Ozone Datasets) overpass data, where temporal selection of each NOAA/2 or Nimbus satellite observations is done through quality assurance, orbit position and errors analysis, thus creating a merged time series of the SBUV V8.6 ozone profiles. The period of each satellite operation and the overlap periods are presented in Fig. 3a. NOAA-16 (from 2007) and NOAA-17 (from 2010) are not used due to rapidly drifting orbits. The left panel in Fig. 3b compares the mean ozone profile for SBUV/2 V8.6 and Umkehr data over Syowa, the right panel shows the mean bias, with the error bars representing one standard deviation. In summary, mean Umkehr ozone is lower than the homogenized SBUV by about 6 % in the stratosphere, and is lower than SBUV by about 1 % in the troposphere, and it shows good agreement with Umkehr. The overall long term trend and seasonal variation agree in both the Umkehr and SBUV records when using only matched days.

The time series of upper stratospheric ozone from the homogenized Nimbus-7 and NOAA SBUV (/2) V8.6 overpass data (±4°, 24 h) show a relative difference in good agreement with Syowa station data. For this analysis we interpolated adjusted SBUV ozone profiles that are defined by the 21 pressure level scheme to ten standard Umkehr layers.

Comparisons of the recently released V8.6 MOD dataset with the ground-based instruments are of importance. Since Syowa station is located at high latitude of 69° S,

ACPD
13, 379–435, 2013

Long term changes in the upper stratospheric ozone at Syowa, Antarctica

K. Miyagawa et al.

and is periodically found inside or outside of the polar vortex, it is a unique data set for data validation. Since the shape of the Antarctic vortex is not ideally symmetrical, we compare zonally averaged and OP data to show how the location of the vortex affected Syowa data over the last 30 yr of observations. During our research (not shown here), we assessed differences between zonal mean (ZM) and overpass (OP) data sets of two versions of SBUV time series matched to Syowa station geo-location, among these are:

1) Zonal mean of V8.6 (5-degrees zonal band centered at 70° S) time series that are statistically adjusted (Long and Wild, private communications, 2012) (further referred as V8.6IS ZM70S).

2) Zonal mean V8.6 MOD dataset (65–70° S and 70–75° S) (Bhartia et al., 2012; McPeters et al., 2012; DeLand et al., 2012) (referred as V8.6MOD ZM6570S, V8.6MOD. ZM7075S).

3) V8.6 station overpass data from the MOD dataset (S. Frith, NASA/Goddard, private communications, 2012) (V8.6MOD OP).

The monthly mean time series (see Fig. 4a) shows the difference between ZM (70° S) and OP SBUV V8.6 MOD data in layer 8 + 9 + 10 (ozone column above 4 hPa pressure level). The long-term change in the difference is clearly seen in the plot. The averaged offset between datasets is about 7 %, while during N17 and N18 operational period (from 2003) ZM data are very close to the OP ozone values (black fitting curve in Fig. 4a represents running mean). This result suggests that the long-term ozone changes in Syowa OP are not in agreement with long-term time series of ZM. However, both ZM data sets whenever created by statistical adjustment from individual satellites (V8.6IS ZM70S) or merged by temporal selection of satellites (V8.6MOD ZM) (not shown) are generally found to agree in time dependency of ozone zonal mean changes at 70° S. Figure 4b shows the time series of the difference between 65–70° S and 70–75° S zonal averages relative to the OP data. It appears that comparisons between 70–75° S ZM and OP data are on average in a better agreement than 65–70° S ZM results, even though the latter ones are geographically closer to 69° S location of Syowa station.

ACPD
13, 379–435, 2013

Since ozone over Syowa is periodically affected by the location of the vortex, and the vortex position in spring time has known to be slowly shifting relative to the station (Hassler et al., 2011), the use of the zonally averaged data is not appropriate for comparisons with the ground-based stations observations over the extended periods of time. We limit further analysis to OP on matched days.

Figure 5 shows the relation of SBUV OP and Umkehr data for annual mean and two seasons.

Agreement between Umkehr and OP annual mean data is shown as scatter plot in Fig 5a. A good match is indicated by the linear fit with 1.00 slope, no bias (offset = 0.0 DU), and 0.78 correlation. We also compared data for spring (August through November) and summer (December through April) seasons (Fig. 5b, c, respectively). The correlation coefficient is lower for comparisons during the summer season ($R = 0.64$), while it is higher during the spring season comparisons ($R = 0.85$). We also found a difference in data agreement when comparisons are separated in two time periods: prior and after 2001 (see Table 3). We found that the offset between the satellite and Umkehr data during spring season did not change significantly between two time periods. However, in the earlier period the slope was significantly higher as compared to the comparisons during the second period, while the correlation was higher in the first period. The first time period is characterized by sporadic Umkehr measurements and high variability due to effects of ENSO and aerosols from Pinatubo volcanic eruption. Results for the summer season show that both slope and correlation were reduced in the second period of comparisons. The reduction in the correlation could be related to the smaller range in ozone variability and not necessarily to the errors in the data (Fioletov et al., 2006). The V8.6 SBUV satellite dataset appears to eliminate most of the internal offsets between satellites. Thus, the V8.6 MOD time series of upper stratospheric ozone are found to be in qualitative agreement with Syowa station Umkehr ozone time series. The summary of the correlation of between SBUV and Umkehr data taken on the same day for individual months and seasonal averages is shown in Table 3.

Figure 6 shows the relationship between the long-term change in ozone in layer 8 + (above 4 hPa or 40 km) and the EESC curve (Polar 2). The annual cycle, effects of solar activity and QBO signals were removed from the data prior to the ozone record trend analysis for Umkehr and SBUV (/2). The remaining large scale variability in the residual ozone time series tends to correlate with the ENSO signal (see blue-shaded vertical rectangles in Fig. 4 that indicate strong El Nino years). The offset of SBUV ozone is adjusted to the mean value (1977–2001) of Umkehr. The annual trend from 1977 to 2001 is larger in Umkehr (−7.7 % $decade^{-1}$) than in SBUV V8.6 (−5.0 % $decade^{-1}$). A large ozone variation appears to suggest a relation with ENSO events. V8.6 trends are in closer agreement with the Umkehr-derived trend as compared to V8 SBUV trend. The long-term change for both versions of SBUV data shows close agreement with changes indicated by the Polar 2 EESC curve.

4 Discussion

To analyze long-term changes in the ozone record at Syowa station we need to understand the variability contributed by mechanisms other than chemical processes related to the ODS concentrations in the stratosphere. After analyzing explanatory parameters that were included in the model (described at the end of Sect. 3.2), we determined that all proxies were required to produce the best fit (the smallest residuals). Figure 7 shows long-term variations of ozone amount in annual mean and spring/summer seasons, and cumulative sum (CUSUM). Results are shown for ozone changes in layer 8 + (above 4 hPa or 40 km) and layer 4 (64–32 hPa or ∼ 20–25 km) that represent upper and middle stratospheric layers respectively. In order to eliminate natural variability associated with seasonal variations, solar activity and QBO, a statistical model (see above) is fitted in the time-series and all explanatory variables (AOD, SAM, ENSO, Heat Flux and EqLat) are removed from the data.

4.1 Trend using all the explanatory variables

In this section, we examine the results of a long-term trend model from the data set with all the explanatory variables included. The left panels in Fig. 7a–d indicate the long-term trend of the ozone in the annual mean, spring and summer season. Symbols in plots (red circles) display the evolution of annual (upper panels) and seasonal (austral spring and summer) averages spanning three decades of observation. The black dashed line shows the linear trend fit for the data record between 1977 and 2001. The shaded area shows 95 % confidence level of the fit. The inflection point in the time series or the reverse in the ozone depletion is selected in 2001 corresponding to the 2001 maximum in the EESC Polar 2 curve (as discussed above). The first part of the record between 1977 and 2001 is then analyzed for linear trend. The difference in ozone trends between upper (panel a) and middle (panel b) stratosphere is clearly shown in Fig. 7. The linear trends derived from annual (upper panels) and seasonal (mid and bottom panels) averages in upper stratosphere are found to be the largest in the spring and summer season, while in the middle stratosphere, the spring season trends are the largest (Fioletov and Shepherd, 2005). This indicates that different processes appear to affect long-term variability in the middle and upper stratosphere.

Long-term trend analyses of the Umkehr (a) and SBUV (b) time-series of ozone changes in the upper stratosphere (layer $8+9+10$) during the first half of the record (prior to 2002) estimate a linear ozone decrease in the annual mean (−8.8 and −5.6 % decade^{-1} respectively), summer (−8.6 and −6.2 % decade^{-1}) and spring (−10.4 and −6.3 % decade^{-1}) seasonal averages. It is noticed that Umkehr and SBUV OP based trends do not agree, even within the uncertainties of the fit. Sparseness and higher variability in the Umkehr data could be partially responsible for the disagreement between two datasets. Also, DeLand et al. (2012) notes that diurnal ozone changes in the upper stratosphere (2–8 %) may not be completely accounted for when the time series of ozone measurements from different satellites are combined to create MOD V8.6 time series (Boyd et al., 2007; Haefele et al., 2008). The NOAA-2 satellites are placed on the drifting orbits and effectively collect data over the ground station at various local times. This could be causing offsets when records from different satellites are spliced to create long-term time series, which can affect the long-term trends. Analysis and correction for the diurnal ozone changes need further investigation.

For the second half of the record, after 2002, the spring-time averaged ozone appears to decrease slightly further until ~2006, and then shows steady increase through the end of 2010. At the same time in the summer season, ozone depletion appears to have leveled off after 2001. When the long-term trends of stratospheric ozone are compared between spring and summer, the rate of ozone depletion in the summer has significantly changed from the linear decline.

Results of ozone trend analysis in the lower stratosphere, where most of the heterogeneous chemical processes take place, are as follows. The long-term variability in monthly and seasonal averages of Umkehr and SBUV derived ozone in layer 4 (between 63 and 32 hPa pressure levels) are shown for the annual mean, spring and summer seasons in the left side panels of the Fig. 7c, d respectively. The long-term annual averaged ozone time-series is found to decrease rapidly in the first half of the Umkehr and SBUV records (-15.8 and -15.2 % decade^{-1} respectively), while both data sets show a much different trend in the second half of the record. The seasonally separated long-term trends show the strongest decrease in lower stratospheric ozone in the springtime during the first half of the record (-41.4 and -37.8 % decade^{-1}) and show little change, appearing rather flat, in the second half of the record; in contrast, summer time ozone does not show any significant long-term changes in either the first or second half of the record. These features agree with changes observed in the total ozone column record (WMO, 2007). As discussed in Salby et al. (2012), total ozone record at South Pole shows strong coherence with planetary wave forcing, which is consistent with a similar coherence of springtime temperature, which also modulates PSC formation. Extremely low ozone concentrations were observed in all layers (except for layer 1) at Southern Hemisphere stations (Syowa, Lauder etc.) in 2006, which was considered as an "unusual" behavior in the long-term record (Miyagawa and Sasaki, 2009).

The record low ozone was also accompanied by unusually low lower stratospheric temperatures (http://www.cpc.ncep.noaa.gov/products/stratosphere/winter_bulletins/sh_06/). The polar vortex in 2006 was larger than usual and low temperatures in the lower stratosphere persisted into November. Moreover, an extremely large decrease in the upper stratospheric ozone (layer 8+) was observed in spring over the last 6 yr (2006–2011), with low ozone values continuing to be observed in the following summers. Prior to the beginning of systematic measurements at Syowa Umkehr measurements were collected in the Antarctic region for several years at Faraday (65.0° S), King Baudouin (70.0° S) and Halley (73.5° S) stations. Symbols shown on the left side of the plot in Fig. 7 provide the reference seasonal ozone value averaged from 1957 to 1972 that is representative of the "pre-ozone hole" levels over Antarctica. An acceptable agreement is found for seasonal ozone averages measured at the three historical Antarctic stations and Syowa station. The ozone trend for each Umkehr layer derived from the Syowa record is summarized in Table 4.

4.2 CUSUM analysis

The cumulative sum (CUSUM) of Umkehr and SBUV time series ozone residuals can be used for systematic assessment of the change in the trend (Newchurch et al., 2003; Yang et al., 2006). The right panels in Fig. 7a–d show the CUSUM in the annual mean, spring and summer seasons. The CUSUM of residual assesses the agreement between the tendency observed in the data and the predictions of the two Goddard-modeled EESC curves (Polar 2–5.5 yr of mean age-of-air, and Polar 3–10 yr of mean age-of-air) that represent the rate of the ODS-related ozone destruction and recovery as function of time. A linear trend is calculated from the time series of residuals of the statistical model (includes all but EESC proxies) fit into ozone data selected between 1977 and 2001. The linear fit is then extended after 2001, and the departure of the residual data from the linear fit is plotted as cumulative change in ozone levels relative

ACPD
13, 379–435, 2013

to the predicted ozone depletion after 2001. An envelope of the 95 % confidence level is shown. The change from the linear forecast is therefore clearly detectable.

Systematic positive CUSUM is observed after the turning point in 2001 for the annual mean, spring, and summer subset of the data. CUSUM is found above a 95 % confidence level (dashed lines). When the two EESC curves are compared to the CUSUM of Umkehr ozone in upper stratosphere (layer 8 + 9 + 10), Polar 2 (blue line) curve indicates faster recovery as compared to the annual and spring season Umkehr data estimates, while summer season data appear to be following Polar 2 curve prediction of ozone recovery. The Polar 3 curve (green line), which has a maximum in 2008, shows closer fit to the results of the spring time Umkehr CUSUM data between 2006 and 2008. Therefore, the change in the Umkehr ozone trend most likely happens later than predicted by the Polar 2 EESC curve (2001). The CUSUM analyses of the SBUV data appear to follow the Polar 3 curve (green) until ~ 2006 and then start to merge to the predictions of Polar 2 curve (blue line). Conversely, in layer 4, systematic positive CUSUM is found after the turning point in 2001 in annual mean and the spring season data. The Annual mean and spring CUSUM is above a 95 % confidence level, and the increase in the summer season data is within the confidence limits. It appears that both Umkehr and SBUV OP CUSUM analysis of ozone data in layer 4 selected during the spring season show a close agreement with the ozone recovery rate predicted by Polar 2 curve (blue).

4.3 Ozone variability

The relation between ozone and atmospheric temperature is important for quantifying the rates of ozone destruction. We analyzed relation between ozone and temperature variability in the upper stratosphere using the temperature re-analysis data sets from the MERRA stratospheric analysis. Furthermore, the correlation between Southern Annular Mode (SAM), El Niño Southern Oscillations (ENSO), and long-term temperature variability are also examined.

ACPD
13, 379–435, 2013

After removing solar activity and QBO, ozone layer 8 shows clear relationships to temperature, ENSO, and SAM. Ozone has a negative correlation with temperature, and a positive correlation with the ENSO index (Fig. 8). The high correlation appears clearly in the late spring period (October to December) when the solar elevation is relatively high. In November, the clear negative correlation between ozone and the monthly mean temperature variability at 2 hPa is the most remarkable. Monthly averages of ozone (layer 8) and temperature at 2 hPa for the month of November show a strong correlation between a decline in temperature and the increase in ozone that is based on the photochemical ozone destruction cycle. There appears to have been an especially high correlation ($R = 0.9$) in the last 10 yr. The relation between temperature (2-hPa) and ozone (layer 8) has clear negative slope ($-0.17\,\mathrm{DU\,K^{-1}}$). The temperature of the middle and upper stratosphere over middle latitudes decreased over the past several decades (Randel et al., 2009; Stolarski et al., 2010). At the same time, the rate of temperature decrease in the Polar lower stratosphere (altitude 10–25 km) is the largest as determined from the radio sonde data at Syowa station (Sato and Motoyoshi, 2008). Although caution is required when using the JMA radiosonde data record from Syowa since there have been four types of instruments used since 1969. The decrease in middle and low stratospheric temperature in Syowa record begins in 1990s, and is amplified by the increase in stratospheric ozone destruction. However, above 27 km (~ 15 hPa), temperature continues to increase (Fig. 9a–d). In the MERRA data, change of the temperature in the upper stratosphere shows the maximum trend during winter, which appears to have decreased in the 2000s (Fig. 9e).

The studies of Lu et al. (2009) and Kuroda et al. (2005) showed that the 11-yr solar cycle and associated change had detectable effects on the stratospheric and tropospheric circulation. In this study, we examine the relationship of the high solar activity years (HS) to the SAM index. High correlation is seen between ozone and SAM from separated HS years (1978–1982, 1988–1992, and 1998–2002). A strong correlation was found between upper stratospheric ozone and the SAM proxy during periods with high solar activity. The correlation coefficient for ozone and SAM in layer 6–7 in Novem-

ACPD
13, 379–435, 2013

ber is 0.9. Such a high correlation in HS continues from spring to summer from the troposphere to the upper stratosphere (Fig. 10a). The relationships of ozone to the Heat Flux (55–75° S mean, 1–3 waves, downloaded from MERRA web page) and Equivalent Latitude data for Syowa are also analyzed. The MERRA reanalysis data set (Rienecker et al., 2008; Schubert et al., 2008) was used to provide a temperature record at 5 hPa over Syowa and to calculate an Equivalent Latitude trend at several pressure levels during the period from 1979 through 2010. The long-term changes in station's equivalent latitude are derived from MERRA analysis at ~3 hPa and ~50 hPa (Fig. 10b). These data are used to attribute some of the upper and middle stratospheric ozone changes to the changes in vortex position relative to station location. Higher negative values represent a more "poleward" location of the station, that is, the station is closer to the center of the polar vortex. The high correlation of the Southern Hemisphere Annular Mode (SAM) with polar upper stratospheric ozone during years of maximum solar activity points toward a strong relationship between the strength of the Brewer-Dobson circulation and Polar stratospheric ozone recovery. Since the SAM and upper stratospheric ozone are both affected by planetary wave propagation, their correlation reflects their response to the same mechanism, especially during High Solar years. The increase in the downward planetary polar wave driving during austral spring since 1979 (Harnik et al., 2011) is affected by changes in the vortex structure at the upper stratosphere levels and by the delayed breakup of the vortex. Another point to investigate is stronger solar cycle differences in the short UV radiation described by Haigh et al. (2010). The authors show that Solar UV radiation determined from the Solar Radiation and Climate Experiment has a 4–6 times stronger solar cycle signal than at other wavelengths. Simulations (Stiller et al., 2008) suggest that this effect reduces ozone concentrations below 45 km.

The long-term trend of ozone at the Syowa station in the lower stratosphere is found to be in agreement with the expected trend based on EESC Polar 2. However, in the upper stratosphere, the recent ozone changes appear to indicate that ozone recovery follows the ODS decline with rates slower that defined by the EESC Polar 2 curve, but

ACPD
13, 379–435, 2013

faster than predicted by the Polar 3 curve. This results could imply an age of air longer than 5.5 yr for the upper stratosphere over Antarctica and longer ODS transit time from the source regions. Although apparent age of air (10 yr) can be derived from the MIPAS SF6 stratospheric measurements over Antarctica, it is most likely affected by descent of mesospheric SF6-depleted air masses, and thus cannot be used to estimate distribution of stratospheric ODS concentrations (or EESC curve) at Polar region (Ray et al., 2010; Garcia et al., 2011; Hall et al., 2011; Steeler et al., 2012). Thus, the latest analyses of the age of air do not support the choice of 10 yr used in the Polar 3 curve modeling (private communications with Fred Moore and Eric Ray, NOAA, Boulder, CO., March 2012). Another possible explanation is that while the increase in greenhouse gases has raised surface temperatures, the stratosphere has cooled, an effect amplified in the Antarctic by the reduction of ozone by ODS and increase in water vapor and carbon dioxide concentrations, and resultant changes in the radiative absorption balance (Thompson et al., 2011). Temperatures in the upper and middle stratosphere at mid-latitudes have remained constant since the middle of 1990s (WMO, 2007; Steinbrecht et al., 2009). According to Hassler et al. (2011), the change of the dynamics of the Antarctic stratosphere has affected ozone reduction at the Antarctic Syowa station.

5 Conclusions

We have investigated the long-term ozone trend in the upper stratosphere over the Antarctic region using the re-processed Umkehr data. Our research is based on Umkehr observations from the Dobson ozone spectrophotometers that are of the high quality required for detection of significant ozone change (recovery) in relation to the decrease in the ODS concentrations. The long-term variability and trend observed in Umkehr ozone profile data is in good agreement with that seen in the SBUV V8.6 Merged Ozone Dataset (see Sect. 3.4 for details). Several explanatory variables (proxies) are utilized in a statistical model to remove effects of quantifiable atmospheric parameters related to inter-annual and dynamically-driven long-term ozone changes,

ACPD
13, 379–435, 2013

such that the trends related to the ODS levels in the stratosphere can be examined. We also verified that part of the long-term ozone changes over Syowa, even in the upper stratosphere, are associated with the changes in the polar vortex position and persistence relative to the geophysical location of Syowa station (Hassler et al., 2011), and that this effect can be attributed in the statistical model using equivalent latitude data at corresponding atmospheric pressure levels. The middle stratospheric ozone trend is found to closely follow the pattern suggested by the polar 2 EESC curve that is currently recommended by the Ozone Assessment (2010) for analysis of data in polar region (5.5 yr). However, at the higher altitudes (to pressure lower than 4 hPa) ozone recovery in Syowa data appears to be delayed (see Fig. 11). Ozone in the upper stratosphere could be affected by a longer transport time. A better fit to Syowa observed ozone variability in the upper stratosphere is obtained using the EESC curve associated with somewhat older age of air (between 6 and 10 yr). Results of the analysis presented in this paper suggest that Syowa's ozone record in the upper stratosphere has not yet reached the second stage of ozone recovery (WMO, 2007; Yang et al., 2008). The Syowa record indicates a statistically significant decrease between 1977 and 2001; after 2000, however, while the stratospheric ozone record essentially remains flat even after the growth of the ODS concentrations has stopped (WMO, 2011). This leveling off of the ozone values in the last ten years suggests continuing ozone destruction caused by a possible delay in the transport of the ODS to the Antarctic upper stratosphere. A recent paper by Stiller et al. (2012) analyzed the MIPAS satellite SF_6 data and estimated an increase in BDC, but also a weakening of the subtropical and polar mixing barriers, meaning a reduction in the strong gradient in the age of air along the edge of the stratospheric jets. The authors find that the changes in the age of air during the 2002–2010 time periods vary between Northern and Southern Hemispheres, as well as between middle, tropical and high latitude regions. The findings of the paper point to differences between lower, middle and upper stratospheric transport processes. For the southern polar upper stratosphere Stiller et al. (2012) find a positive linear increase in the age of air that is larger than published by Engel et al. (2009). Further analysis of the processes

ACPD
13, 379–435, 2013

that could affect analysis of the MIPAS SF_6 data are needed in order to understand the dynamical processes that affect temperature, wave breaking and descent of mesospheric ozone in the polar upper stratosphere in the winter season. Another important process that can contribute to ozone variability in upper stratosphere is the solar flux cycle. Several publications in recent years described potential changes observed in the UV and visible solar flux spectra when transitioning between the maximum and the minimum stages in the solar cycle and associated effects on stratospheric temperature and photochemical processes (Haigh et al., 2010; Oberländer et al., 2012). These papers indicate the importance of understanding the long-term changes in photochemical processes that lead to the production of stratospheric ozone (Haigh et al., 2010). The last Solar cycle maximum was observed in 2000–2002, and the sun's activity declined until December 2009. This longer than usual minimum of the solar cycle could be one factor contributing to the delay in ozone recovery in the upper stratosphere where photochemical processes dominate over dynamical processes. Haigh et al. (2010) showed that an apparent decline of as much as 0.7 % in stratospheric ozone values near 4 hPa between 2004 and 2007 was actually associated with an ozone decrease near 1.2 % when the spectral changes of the solar cycle were taken into account. With the continuation of observations of ozone over the southern polar regions, it will be possible to determine which processes play the most important role and how the climate changes will affect ozone in the future.

Acknowledgements. We would like to thank Eric Beach of NOAA/NESDIS regarding the analysis of satellite, and Chiaki Kobayashi of the Meteorological Research Institute and Toshiyuki Sakurai of Ozone Layer Monitoring Office, Japan Meteorological Agency regarding the analysis of Umkehr observation. In addition, we thank the members of Japanese Antarctic Research Expedition for the continuous long-term ozone field observations. Work at the Jet Propulsion Laboratory, California Institute of Technology was done under contract with the National Aeronautics and Space Administration.

ACPD
13, 379–435, 2013

References

Appenzeller, C., Weiss, A. K., and Staehelin, J.: North Atlantic oscillation modulates total ozone winter trends, Geophys. Res. Lett., 27, 1131–1134, 2000.

Arblaster, J. M. and Meehl, G. A.: Contributions of external forcings to southern annular mode trends, J. Climate, 19, 2896–2905, 2006.

Bhartia, P. K., McPeters, R. D., Mateer, C. L., Flynn, L. E., and Wellemeyer, C. G.: Algorithm for the estimation of vertical profiles from the backscattered ultraviolet technique, J. Geophys. Res., 101, 18793–18806, 1996.

Bhartia, P. K., McPeters, R. D., Flynn, L. E., Taylor, S., Kramrova, N. A., Frith, S., Fisher, B., and DeLand, M.: Solar Backscatter UV (SBUV) total ozone and profile algorithm, Atmos. Meas. Tech. Discuss., 5, 5913–5951, doi:10.5194/amtd-5-5913-2012, 2012.

Boyd, I. S., Parrish, A. D., Froidevaux, L., von Clarmann, T., Kyrölä, E., Russell III, J. M., and Zawodny, J. M.: Groundbased microwave ozone radiometer measurements, compared with Aura-MLS v2.2 and other instruments at two network for detection of atmospheric composition change sites, J. Geophys. Res., 112, D24S33, doi:10.1029/2007JD008720, 2007.

Butchart, N. and Remsberg, E. E.: The area of the stratospheric polar vortex as a diagnostic for tracer 5 transport on an isentropic surface, J. Atmos. Sci., 43, 1319–1339, 1986.

DeLand, M. T., Taylor, S. L., Huang, L. K., and Fisher, B. L.: Calibration of the SBUV version 8.6 ozone data product, Atmos. Meas. Tech., 5, 2951–2967, doi:10.5194/amt-5-2951-2012, 2012.

Dhomse, S., Weber, M., and Burrows, J.: The relationship between tropospheric wave forcing and tropical lower stratospheric water vapor, Atmos. Chem. Phys., 8, 471–480, doi:10.5194/acp-8-471-2008, 2008.

Diaz, H. F. and Markgraf, V.: El Niño: Historical and Paleoclimatic Aspects of the Southern Oscillation. Cambridge University Press, 476 pp., 1992.

Douglass, A. R., Stolarski, R. S., Strahan, S. E., and Polansky, B. C.: Sensitivity of Arctic ozone loss to polar stratospheric cloud volume and chlorine and bromine loading in a chemistry and transport model, Geophys. Res. Lett., 33, L17809, doi:10.1029/2006GL026492, 2006.

Douglass, A. R., Stolarski, R. S., Schoeberl, M. R., Jackman, C. H., Gupta, M. L., Newman, P. A., Nielsen, J. E., and Fleming, E. L.: Relationship of loss, mean age of air and the distribution of CFCs to stratospheric circulation and implications for atmospheric lifetimes, J. Geophys. Res., 113, D14309, doi:10.1029/2007JD009575, 2008.

Engel, A., Möbius, T., Bönisch, H., Schmidt, U., Heinz, R., Levin, I., Atlas, E., Aoki, S., Nakazawa, T., Sugawara, S., Moore, F., Hurst, D., Elkins, J., Schauffler, S., Andrews, A., and Boering, K.: Age of stratospheric air unchanged within uncertainties over the pat 30 years, Nat. Geosci., 2, 28–31, 2009.

Farman, J. C., Gardiner, B. G., and Shanklin, J. D.: Large losses of total ozone in Antarctica reveal seasonal ClO_x/NO_x interaction, Nature, 315, 207–210, 1985.

Finger, F. G., Gelman, M. E., Wild, J. D., Chanin, M. L., Hauchecorne, A., and Miller, A. J.: Evaluation of NMC upper-stratospheric temperature analyses using rocketsonde and lidar data, B. Am. Meteorol. Soc., 74, 789–799, 1993.

Fioletov, V. E. and Shepherd, T. G.: Summertime total ozone variations over middle and polar latitudes, Geophys. Res. Lett., 32, L04807, doi:10.1029/2004GL022080, 2005.

Fioletov, V. E., Tarasick, D. W., and Petropavlovskikh, I.: Estimating ozone variability and instrument uncertainties from SBUV(/2), ozonesonde, Umkehr, and SAGE II measurements: short-term variations, J. Geophys. Res., 111, D02305, doi:10.1029/2005JD006340, 2006.

Fogt, R. L. and Bromwich, D. H.: Decadal variability of the ENSO teleconnection to the high-latitude south Pacific governed by coupling with the southern annular mode*, J. Climate, 19, 979–997, 2006.

Fogt, R. L., Perlwitz, J., Pawson, S., and Olsen, M. A.: Intra-annual relationships between polar ozone and the SAM, Geophys. Res. Lett., 36, L04707. doi:10.1029/2008GL036627, 2009.

Garcia, R. R. and Randel, W. J.: Acceleration of the Brewer-Dobson circulation due to increases in greenhouse gases, J. Atmos. Sci., 65, 2731–2739, doi:10.1175/2008JAS2712.1, 2008.

Garcia, R. R., Randel, W. J., and Kinnison, D. E.: On the determination of age of air trends from atmospheric trace species, J. Atmos. Sci., 68, 139–154, 2011.

Garcia-Herrera, R., Calvo, N., Garcia, R. R., and Giorgetta, M. A.: Propagation of ENSO temperature signals into the middle atmosphere: a comparison of two general circulation models and ERA-40 reanalysis data, J. Geophys. Res., 111, D06101, doi:10.1029/2005JD006061, 2006.

Garfinkel, C. I. and Hartmann, D. L.: Effects of the El Niño – Southern Oscillation and the Quasi-Biennial Oscillation on polar temperatures in the stratosphere, J. Geophys. Res., 112, D19112, doi:10.1029/2007JD008481, 2007.

Gelman, M. E.: Stratospheric monitoring with TOVS data, Palaeogeogr. Palaeocl., 90, 75–78, 1991.

ACPD

13, 379–435, 2013

Götz, F. W. P., Meetham, A. R., and Dobson, G. M. B.: The vertical distribution of ozone in the atmosphere, Proc. R. Soc. Lon. Ser. A, 145, 416–443, 1934.
Haefele, A., Hocke, K., Kämpfer, N., Keckhut, P., Marchand, M., Bekki, S., Morel, B., Egorova, T., and Rozanov, E.: Diurnal changes in middle atmospheric H_2O and O_3: observations in the Alpine region and climate models, J. Geophys. Res., 113, D17303, doi:10.1029/2008JD009892, 2008.
Haigh, J. D. and Roscoe, H. K.: Solar influences on polar modes of variability, Meteorol. Z., 15, 371–378, 2006.
Haigh J. D., Winning, A. R., Toumi, R., and Harder, J. W.: An influence of solar spectral variations on radiative forcing of climate, Nature, 467, 696–699, 2010.
Hall, B. D., Dutton, G. S., Mondeel, D. J., Nance, J. D., Rigby, M., Butler, J. H., Moore, F. L., Hurst, D. F., and Elkins, J. W.: Improving measurements of SF_6 for the study of atmospheric transport and emissions, Atmos. Meas. Tech., 4, 2441–2451, doi:10.5194/amt-4-2441-2011, 2011.
Hamilton, K.: Effects of an imposed quasi-biennial oscillation in a comprehensive troposphere–stratosphere-mesosphere general circulation model, J. Atmos. Sci., 55, 2393–2418, 1998.
Harnik, N., Perlwitz, J., and Shaw, T. A.: Observed decadal changes in downward wave coupling between the stratosphere and troposphere in the southern hemisphere, J. Climate, 24, 4558–4569, 2011.
Hassler, B., Bodeker, G. E., Solomon, S., and Young, P. J.: Changes in the polar vortex: effects on Antarctic total ozone observations at various stations, Geophys. Res. Lett., 38, L01805, doi:10.1029/2010GL045542, 2011.
Hitchman, M. H. and Rogal, M. J.: Seasonal and ENSO Influences of Tropical Convection on SH Ozone During the Winter to Spring Transition, in: Fall Meeting 2010, American Geophysical Union, abstract #A51B-0091, 2010.
Hoskins, B. J. and Karoly, D. J.: The steady linear response of a spherical atmosphere to thermal and orographic forcing, J. Atmos. Sci., 38, 1179–1196, 1981.
Hu, Y. and Fu, Q.: Stratospheric warming in Southern Hemisphere high latitudes since 1979, Atmos. Chem. Phys., 9, 4329–4340, doi:10.5194/acp-9-4329-2009, 2009.
Ialongo, I., Sofieva, V., Kalakoski, N., Tamminen, J., and Kyrölä, E.: Ozone zonal asymmetry and planetary wave characterization during Antarctic spring, Atmos. Chem. Phys., 12, 2603–2614, doi:10.5194/acp-12-2603-2012, 2012.

Jiang, X., Pawson, S., Camp, C. D., Nielsen, E., Shia, R., Liao, T., Jeev, K., Limpasuvan, V., and Yung, Y. L.: Interannual variability and trends in extratropical ozone. Part II: Southern Hemisphere, J. Atmos. Sci., 65, 3030–3041, 2008.
Krzyścin, J. W. and Rajewska-Więch, B.: Trends in the ozone vertical distribution from the Umkehr observations at Belsk 1963–2007, Int. J. Remote Sens., 30, 3917–3926, doi:10.1080/01431160902821866, 2009.
Kuroda, Y. and Kodera, K.: Solar cycle modulation of the Southern Annular Mode, Geophys. Res. Lett., 32, L13802, doi:10.1029/2005GL022516, 2005.
Kuroda, Y. and Yamazaki, K.: Influence of the solar cycle and QBO modulation on the Southern Annular Mode, Geophys. Res. Lett., 37, L12703, doi:10.1029/2010GL043252, 2010.
Kushner, P. J., Held, I. M., and Delworth, T. L.: Southern Hemisphere atmospheric circulation response to global warming, J. Climate, 14, 2238–2249, 2001.
L'Heureux, M. L. and Thompson, D. W. J.: Observed relationships between the El Niño-Southern Oscillation and the extratropical zonal-mean circulation, J. Climate, 19, 276–287, 2006.
Li, F., Stolarski, R. S., and Newman, P. A.: Stratospheric ozone in the post-CFC era, Atmos. Chem. Phys., 9, 2207–2213, doi:10.5194/acp-9-2207-2009, 2009.
Li, F., Newman, P. A., and Stolarski, R. S.: Relationships between the Brewer-Dobson circulation and the southern annular mode during austral summer in coupled chemistry-climate model simulations, J. Geophys. Res., 115, D15106, doi:10.1029/2009JD012876, 2010.
Livesey, N. J., Read, W. G., Froidevaux, L., Waters, J. W., Santee, M. L., Pumphrey, H. C., Wu, D. L., Shippony, Z., and Jarnot, R. F.: The UARS Microwave Limb Sounder version 5 data set: theory, characterization, and validation, J. Geophys. Res., 108, 4378, doi:10.1029/2002JD002273, 2003.
Lu, H., Gray, L. J., Baldwin, M. P., and Jarvis, M. J.: Life cycle of the QBO modulated 11-year solar cycle signals in the Northern Hemispheric winter, Q. J. Roy. Meteorol. Soc., 135, 1030–1043, 2009.
Lu, H., Jarvis, M. J., Gray, L. J., and Baldwin, M. P.: High- and low-frequency 11-year solar cycle signatures in the Southern Hemispheric, Q. J. Roy. Meteorol. Soc., 137, 1641–1656, 2011.
Mäder, J. A., Staehelin, J., Brunner, D., Stahel, W. A., Wohltmann, I., and Peter, T.: Statistical modeling of total ozone: Selection of appropriate explanatory variables, J. Geophys. Res., 112, D11108, doi:10.1029/2006JD007694, 2007.

ACPD
13, 379–435, 2013

Manney, G. L., Zurek, R. W., Gelman, M. E., Miller, A. J., and Nagatani, R.: The anomalous arctic lower stratospheric polar vortex of 1992–1993, Geophys. Res. Lett., 21, 2405–2408, 1994.
Manney, G. L., Michelsen, H. A., Santee, M. L., Gunson, M. R., Irion, F. W., Roche, A. E., and Livesey, N. J.: Polar vortex dynamics during spring and fall diagnosed using trace gas observations from the atmospheric trace molecule spectroscopy instrument, J. Geophys. Res., 104, 18841–18866, 1999.
Marshall, G. J.: Trends in the Southern Annular Mode from observations and reanalyses, J. Climate, 16, 4134–4143, 2003.
McPeters, R. D., Labow, G. J., and Logan, J. A.: Ozone climatological profiles for satellite retrieval algorithms, J. Geophys. Res., 112, D05308, doi:10.1029/2005JD006823, 2007.
McPeters, R. D., Bhartia, P., and Flynn, L.: A 40 year time series of SBUV observations: the version 8.6 processing, in: Quadrennial Ozone Symposium 2012, Toronto, ID5929, 2012.
Miyagawa, K.: Development of automated measuring system for Dobson ozone spectrophotometer, in: XVIII Quadrennial Ozone Symposium, vol. 2, edited by: Bojkov, R. and Visconti, G., Int. Ozone Comm., L'Aquila, Italy, 951–954, 1996.
Miyagawa, K. and Sasaki, T.: Vertical ozone profile by umkehr measurements at Syowa Station, Int. J. Remote Sens., 30, 4043–4053, 2009.
Miyagawa, K., Sasaki, T., Nakane, H., Petropavlovskikh, I., and Evans, R. D.: Reevaluation of long-term Umkehr Data and Ozone profiles at Japanese stations, J. Geophys. Res., 114, D07108, doi:10.1029/2008JD010658, 2009.
Molina, M. J. and Rowland, F. S.: Stratospheric sink for chlorofluoromethanes: chlorine atom catalyzed destruction of ozone, Nature, 810–812, 1974.
Nash, E. R., Newman, P. A., Rosenfield, J. E., and Schoeberl, M. R.: An objective determination of the polar vortex using Ertel's potential vorticity, J. Geophys. Res., 101, 9471–9478, 1996.
Newchurch, M. J., Yang, E. S., Cunnold, D. M., Reinsel, G. C., Zawodny, J. M., and Russell III, J. M.: Evidence for slowdown in stratospheric ozone loss: first stage of ozone recovery, J. Geophys. Res., 108, 4507, doi:10.1029/2003JD003471, 2003.
Newman, P. A., Nash, E. R., and Rosenfield, J. E.: What controls the temperature of the Arctic stratosphere during the spring?, J. Geophys. Res., 106, 19999–20010, 2001.
Newman, P. A., Nash, E. R., Kawa, S. R., Montzka, S. A., and Schauffler, S. M.: When will the Antarctic ozone hole recover?, Geophys. Res. Lett., 33, L12814, doi:10.1029/2005GL025232, 2006.

ACPD
13, 379–435, 2013

Newman, P. A., Daniel, J. S., Waugh, D. W., and Nash, E. R.: A new formulation of equivalent effective stratospheric chlorine (EESC), Atmos. Chem. Phys., 7, 4537–4552, doi:10.5194/acp-7-4537-2007, 2007.
Oberländer, S., Langematz, U., Matthes, K., Kunze, M., Kubin, A., Harder, J., Krivova, N. A., Solanki, S. K., Pagaran, J., and Weber, M.: The influence of spectral solar irradiance data on stratospheric heating rates during the 11 year solar cycle, Geophys. Res. Lett., 39, L01801, doi:10.1029/2011GL049539, 2012.
Oman, L., Waugh, D. W., Pawson, S., Stolarski, R. S., and Newman, P. A.: On the influence of anthropogenic forcings on changes in the stratospheric mean age, J. Geophys. Res., 114, D03105, doi:10.1029/2008JD010378, 2009.
Oman, L. D., Waugh, D. W., Kawa, S. R., Stolarski, R. S., Douglass, A. R., and Newman, P. A.: Mechanisms and feedback causing changes in upper stratospheric ozone in the 21st century, J. Geophys. Res., 115, D05303, doi:10.1029/2009JD012397, 2010.
Pan, L. L., Kunz, A., Homeyer, C. R., Munchak, L. A., Kinnison, D. E., and Tilmes, S.: Commentary on using equivalent latitude in the upper troposphere and lower stratosphere, Atmos. Chem. Phys., 12, 9187–9199, doi:10.5194/acp-12-9187-2012, 2012.
Perlwitz, J. and Harnik, N.: Downward coupling between the stratosphere and troposphere: the relative roles of wave and zonal mean processes, J. Climate, 17, 4902–4909, doi:10.1175/JCLI-3247.1, 2004.
Perlwitz, J., Pawson, S., Fogt, R. L., Nielsen, J. E., and Neff, W. D.: Impact of stratospheric ozone hole recovery on Antarctic climate, Geophys. Res. Lett., 35, L08714, doi:10.1029/2008GL033317, 2008.
Petropavlovskikh, I., Bhartia, P. K., and DeLuisi, J.: New Umkehr ozone profile retrieval algorithm optimized for climatological studies, Geophys. Res. Lett., 32, L16808, doi:10.1029/2005GL023323, 2005.
Petropavlovskikh, I., Evans, R. D., McConville, G., Miyagawa, K., and Oltmans, S.: Effect of the out-of-band stray light on the retrieval of the Umkehr Dobson ozone profiles, Int. J. Remote Sens., 30, 24, 6461–6482, 2009.
Poberaj, C. S., Staehelin, J., and Brunner, D.: Missing stratospheric ozone decrease at Southern Hemisphere middle latitudes after Mt. Pinatubo: a dynamical perspective, J. Atmos. Sci., 68, 1922–1945, 2011.
Randel, W. J.: Study of planetary waves in the southern winter troposphere and stratosphere. Part 1: Wave structure and vertical propagation, J. Atmos. Sci., 44, 917–935, 1987.

ACPD
13, 379–435, 2013

Randel, W. J.: The seasonal evolution of planetary-waves in the southern-hemisphere stratosphere and troposphere, Q. J. Roy. Meteorol. Soc., 114, 1385–1409, 1988.
Randel, W. J., Shine, K. P., Austin, J., Barnett, J., Claud, C., Gillett, N. P., Keckhut, P., Langematz, U., Lin, R., Long, C., Mears, C., Miller, A., Nash, J., Seidel, D. J., Thompson, D. W. J., Wu, F., and Yoden, S.: An update of observed stratospheric temperature trends, J. Geophys. Res., 114, D02107, doi:10.1029/2008JD010421, 2009.
Ray, E. A., Moore, F. L., Rosenlof, K. H., Davis, S. M., Boenisch, H., Morgenstern, O., Smale, D., Rozanov, E., Hegglin, M., Pitari, G., Mancini, E., Braesicke, P., Butchart, N., Hardiman, S., Li, F., Shibata, K., and Plummer, D. A.: Evidence for changes in stratospheric transport and mixing overi the past three decade based on multiple data sets and tropical leaky pipe analysis, J. Geophys. Res., 115, D21304, doi:10.1029/2010JD014206, 2010.
Rienecker, M. M., Suarez, M. J., Todling, R., Bacmeister, J., Takacs, L., Liu, H.-C., Gu, W., Sienkiewicz, M., Koster, R. D., Gelaro, R., Stajner, I., and Nielsen, J. E.: The GEOS-5 data assimilation system – documentation of versions 5.0.1, 5.1.0, and 5.2.0, in: Technical Report Series on Global Modeling and Data Assimilation, NASA/TM-2008-104606, Vol. 27, National Aeronautics and Space Administration, Goddard Space Flight Center, Greenbelt, Maryland 20771, http://gmao.gsfc.nasa.gov/pubs/docs/Rienecker369.pdf, 2008.
Reinsel, G. C., Weatherhead, E. C., Tiao, G. C., Miller, A. J., Nagatani, R. M., Wuebbles, D. J., and Flynn, L. E.: On detection of turnaround and recovery in trend for ozone, J. Geophys. Res., 107, 1–12, 2002.
Reinsel, G. C., Miller, A. J., Weatherhead, E. C., Flynn, L. E., Nagatani, R., Tiao, G. C., and Wuebbles, D. J.: Trend analysis of total ozone data for turnaround and dynamical contributions, J. Geophys. Res., 110, D16306, doi:10.1029/2004JD004662, 2005.
Rosenfield, J. E., Douglass, A. R., and Considine, D. B.: The impact of increasing carbon dioxide on ozone recovery, J. Geophys. Res., 107, 4049, doi:10.1029/2001JD000824, 2002.
Salby, M., Titova, E., and Deschamps, L.: Rebound of Antarctic ozone, Geophys. Res. Lett., 38, L09702, doi:10.1029/2011GL047266, 2011.
Salby, M. L., Titova, E. A., and Deschamps, L.: Changes of the Antarctic ozone hole: controlling mechanisms, seasonal predictability, and evolution, J. Geophys. Res., 117, D10111, doi:10.1029/2011JD016285, 2012.
Sassi, F., Kinnison, D., Boville, B. A., Garcia, R. R., and Roble, R.: Effect of El Niño – Southern Oscillation on the dynamical, thermal, and chemical structure of the middle atmosphere, J. Geophys. Res., 109, D17108, doi:10.1029/2003JD004434, 2004.

ACPD
13, 379–435, 2013

Long term changes in the upper stratospheric ozone at Syowa, Antarctica

K. Miyagawa et al.

Sato, K. and Motoyoshi, Y.: Gravity wave generation around the polar vortex in the stratosphere revealed by 3-hourly radiosonde observations at Syowa Station, J. Atmos. Sci., 65, 3719–3735, doi:10.1175/2008JAS2539.1, 2008.
Schoeberl, M. R., Lait, L. R., Newman, P. A., and Rosenfield, J. E.: The structure of the polar vortex, J. Geophys. Res., 97, 7859–7882, 1992.
Schubert, S., Bosilovich, M., Rienecker, M., Suarez, M., Gelaro, R., Koster, R., Bacmeister, J., Todling, R., Takacs, L., Liu, E., Kim, G.-K., Lucchesi, R., Wu, M.-L., Pegion, P., Lee, M.-I., Chen, J., Bloom, S., Reichle, R., Pawson, S., Stajner, I., Silva, A., Keppenne, C., Gregg, W., and others in the GMAO: Assimilating Earth system observations at NASA: MERRA and beyond, in: Third WCRP International Conference on Reanalysis, Tokyo, Japan, http://wcrp.ipsl.jussieu.fr/Workshops/Reanalysis2008/Documents/V1-104_ea.pdf, 2008.
Shindell, D. T.: Climate and ozone response to increased stratospheric water vapor, Geophys. Res. Lett., 28, 1551–1554, 2001.
Solomon, S.: Stratospheric ozone depletion: a review of concepts and history, Rev. Geophys., 37, 275–316, 1999.
Solomon, S., Garcia, R. R., Rowland, F. S., and Wuebbles, D. J.: On the depletion of Antarctic ozone, Nature, 321, 755–758, 1986.
Solomon, S., Portmann, R. W., Sasaki, T., Hofmann, D. J., and Thompson, D. W. J.: Four decades of ozonesonde measurements over Antarctica, J. Geophys. Res., 110, D21311, doi:10.1029/2005JD005917, 2005.
Son, S.-W., Polvani, L. M., Waugh, D. W., Akiyoshi, H., Garcia, R., Kinnison, D., Pawson, S., Rozanov, E., Shepherd, T. G., and Shibata, K.: The impact of stratospheric ozone recovery on the Southern Hemisphere westerly jet, Science, 320, 1486–1489, doi:10.1126/science.1155939, 2008.
Son, S. W., Gerber, E. P., Perlwitz, J., Polvani, L. M., Gillett, N. P., Seo, K. H., Eyring, V., Shepherd, T. G., Waugh, D., Akiyoshi, H., Austin, J., Baumgaertner, A., Bekki, S., Braesicke, P., Brühl, C., Butchart, N., Chipperfield, M. P., Cugnet, D., Dameris, M., Dhomse, S., Frith, S., Garny, H., Garcia, R., Hardiman, S. C., Jöckel, P., Lamarque, J. F., Mancini, E., Marchand, M., Michou, M., Nakamura, T., Morgenstern, O., Pitari, G., Plummer, D. A.,Pyle, J., Rozanov, E., Scinocca, J. F., Shibata, K., Smale, D., Teyssèdre, H., Tian, W., and Yamashita, Y.: Impact of stratospheric ozone on Southern Hemisphere circulation change: a multimodel assessment, J. Geophys. Res., 115, D00M07, doi:10.1029/2010JD014271, 2010.

Steinbrecht, W., Claude, H., Köhler, U., and Hoinka, K. P.: Correlations between tropopause height and total ozone: implications for long-term changes, J. Geophys. Res., 103, 19183–19192, 1998.

Steinbrecht W., Claude, H., Schönenborn, F., McDermid, I. S., Leblanc, T., Godin-Beekmann, S., Keckhut, P., Hauchecorne, A., Van Gijsel, J. A. E., Swart, D. P. J., Bodeker, G. E., Parrish, A., Boyd, I. S., Kämpfer, N., Hocke, K., Stolarski, R. S., Frith, S. M., Thomason, L. W., Remsberg, E. E., Von Savigny, C., Rozanov, A., and Burrows, J. P.: Ozone and temperature trends in the upper stratosphere at five stations of the network for the detection of atmospheric composition change, Int. J. Remote Sens., 30, 3875–3886, 2009.

Stiller, G. P., von Clarmann, T., Höpfner, M., Glatthor, N., Grabowski, U., Kellmann, S., Kleinert, A., Linden, A., Milz, M., Reddmann, T., Steck, T., Fischer, H., Funke, B., López-Puertas, M., and Engel, A.: Global distribution of mean age of stratospheric air from MIPAS SF_6 measurements, Atmos. Chem. Phys., 8, 677–695, doi:10.5194/acp-8-677-2008, 2008.

Stiller, G. P., von Clarmann, T., Haenel, F., Funke, B., Glatthor, N., Grabowski, U., Kellmann, S., Kiefer, M., Linden, A., Lossow, S., and López-Puertas, M.: Observed temporal evolution of global mean age of stratospheric air for the 2002 to 2010 period, Atmos. Chem. Phys., 12, 3311–3331, doi:10.5194/acp-12-3311-2012, 2012.

Stolarski, R. S., Douglass, A. R., Newman, P. A., Pawson, S., and Schoeberl, M. R.: Relative contribution of greenhouse gases and ozone-depleting substances to temperature trends in the stratosphere: a chemistry–climate model study, J. Climate, 23, 28–42, 2010.

Taguchi, M.: Observed connection of the stratospheric quasi-biennial oscillation with El Niño–Southern Oscillation in radiosonde data, J. Geophys. Res., 115, D18120, doi:10.1029/2010JD014325, 2010.

Thompson, D. W. J. and Solomon, S.: Interpretation of recent Southern Hemisphere climate change, Science, 296, 895–899, 2002.

Thompson, D. W. J., Baldwin, M. P., and Solomon, S.: Stratosphere–troposphere coupling in the Southern Hemisphere, J. Atmos. Sci., 62, 708–715, 2005.

Thompson, D. W. J., Solomon, S., Kushner, P. J., England, M. H., Grise, K. M., and Karoly, D. J.: Signatures of the Antarctic ozone hole in Southern Hemisphere surface climate change, Nat. Geosci., 4, 741–749, doi:10.1038/ngeo1296, 2011.

Turner, J.: Revier the EL NINO–Southern Oscillation and Antarctica, Int. J. Climatol., 24, 1–31, 1994.

ACPD
13, 379–435, 2013

Long term changes in the upper stratospheric ozone at Syowa, Antarctica

K. Miyagawa et al.

Turner, J., Lachlan-Cope, T. A., Colwell, S., Marshall, G. J., and Connolley, W. M.: Significant warming of the Antarctic winter troposphere, Science, 311, 1914–1916, 2006.
Vyushin, D., Fioletov, V. E., and Shepherd, T. G.: Impact of long-range correlations on trend detection in total ozone, J. Geophys. Res., 112, D14307, doi:10.1029/2006JD008168, 2007.
Wang, J., Pawson, S., Tian, B., Yung, Y. L., and Jiang, X.: El Nino-Southern Oscillation in tropical and midlatitude column ozone, J. Atmos. Sci., 68, 1911–1921, 2011.
Waugh, D.: Atmospheric dynamics: The age of stratospheric air, Nat. Geosci., 2, 14–16, doi:10.1038/ngeo397, 2009.
Waugh, D. W. and Hall, T. M.: Age of stratospheric air: theory, observations, and models, Rev. Geophys., 40, 1010, doi:10.1029/2000RG000101, 2002.
Waugh, D. W., Oman, L., Kawa, S. R., Stolarski, R. S., Pawson, S., Douglass, A. R., Newman, P. A., and Nielsen, J. E.: Impacts of climate change on stratospheric ozone recovery, Geophys. Res. Lett., 3, L03805, doi:10.1029/2008GL036223, 2009.
Weiss, A. K., Staehelin, J., Appenzeller, C., and Harris N.: Chemical and dynamical contributions to ozone profile trends of the Payerne (Switzerland) balloon soundings, J. Geophys. Res., 106, 22685–22694, 2001.
Wohltmann, I., Lehmann, R., Rex, M., Brunner, D., and Mäder, J.: A process-oriented regression model for column ozone, J. Geophys. Res.-Atmos., 112, D12304. doi:10.1029/2006JD007573, 2007.
World Meteorological Organization: Scientific assessment of ozone depletion: 1991, Global Ozone Research and Monitoring Project Report, No. 25, Geneva, Switzerland, World Meteorological Organization European Commission, 1992.
World Meteorological Organization (WMO)/United Nations Environment Programme (UNEP): Scientific Assessment of Ozone Depletion: World Meteorological Organization, Global Ozone Research and Monitoring Project, Report No. 50, World Meteorological Organization European Commission, Geneva, Switzerland 2006, 2007.
World Meteorological Organization (WMO)/United Nations Environment Programme (UNEP): Scientific Assessment of Ozone Depletion: World Meteorological Organization, Global Ozone Research and Monitoring Project, Report No. 52, World Meteorological Organization European Commission, Geneva, Switzerland 2010, 2011.
Yang, E.-S., Cunnold, D. M., Salawitch, R. J., McCormick, M. P., Russell III, J., Zawodny, J. M., Oltmans, S., and Newchurch, M. J.: Attribution of recovery in lower-stratospheric ozone, J. Geophys. Res., 111, D17309, doi:10.1029/2005JD006371, 2006.

Yang, E.-S., Cunnold, D. M., Newchurch, M. J., Salawitch, R. J., McCormick, M. P., Russell, J. M., Zawodny, J. M., and Oltmans, S. J.: First stage of Antarctic ozone recovery, J. Geophys. Res.-Atmos., 113, D20308, doi:10.1029/2007JD009675, 2008.
Yoshimatsu, K., Nagata, K., Sakamoto, N., and Fujimoto, T.: Analytical research of the ozone variation factors over Tsukuba, J. Meteorol. Res., 57, 81–94, 2005.
Yuan, X. and Yonekura, E.: Decadal variability in the Southern Hemisphere, J. Geophys. Res., 116, D19115, doi:10.1029/2011JD015673, 2011.
Zanis, P., Maillard, E., Staehelin, J., Zerefos, C., Kosmidis, E., Tourpali, K., and Wohltmann, I.: On the turnaround of stratospheric ozone trends deduced from the reevaluated Umkehr record of Arosa, Switzerland, J. Geophys. Res., 111, D22307, doi:10.1029/2005JD006886, 2006.
Zerefos, C. S., Bais, A. F., Ziomas, I. C., and Bojkov, R. D.: On the relative importance of quasi-biennial oscillation and El Nino/Southern Oscillation in the revised Dobson total ozone records, J. Geophys. Res., 97, 10135–10144, doi:10.1029/92JD00508, 1992.

ACPD
13, 379–435, 2013

Table 1. List of the proxies and sources.

Proxy	Short Hand	Organizational Source	Web Link
Solar Activity Index	SOR	National Astronomical Observatory of Japan	http://www.nao.ac.jp/E/; ftp://solar.nro.nao.ac.jp/pub/norp/data/daily
Quasi-Biennial Oscillation	QBO	Freie Universität Berlin Physics of the Middle Atmosphere (FUB)	produkte/qbo/index.html http://www.geo.fu-berlin.de/en/met/ag/strat/
Southern Hemisphere Annular Mode Index	SAM	British Antarctic Survey	http://www.antarctica.ac.uk/met/gjma/sam.html
El Niño Southern Oscillation	ENSO	NOAA/NWS Climate Prediction Center	http://www.cpc.ncep.noaa.gov/products/analysis_monitoring/ensostuff/ensoyears.shtml
Heat Flux	Heat Flux	NASA: The Modern Era Retrospective-analysis for Research and Applications MERRA	http://acd-ext.gsfc.nasa.gov/Data_services/met/ann_data.html
Equivalent Latitude	EqLat	NASA: Atmospheric Chemistry and Dynamics Laboratory	http://acd-ext.gsfc.nasa.gov/Data_services/met/ann_data.html
Aerosol optical depth	AOD	NASA: Composite	–

ACPD
13, 379–435, 2013

Table 2. RMSD for proxies, and the optimal time-lag. (a) RMSD of the difference from EESC curve (polar 2), and the boldface show minimum of the layer. (b) Optimal time-lag (month) of ozone and proxies is shown.

(a) RMSD by the difference of EESC curve and ozone

	LAYER							
Annual mean	1	2 + 3	4	5	6	7	8	8 + 9 + 10
SOR + QBO1(30 hPa)	0.53	4.98	4.51	3.01	1.49	0.73	0.36	0.46
SOR + QBO2(50 hPa)	0.55	5.05	4.67	3.10	1.47	0.70	0.36	0.46
SOR + QBO3(30 hPa and 50 hPa) + AOD	0.47	4.61	4.44	3.09	1.42	0.68	0.36	0.45
SOR + QBO3 + ENSO	0.47	4.94	4.29	3.13	1.43	0.72	0.37	0.48
SOR + QBO3 + EqLat	0.52	4.95	4.54	3.07	1.38	0.68	0.34	0.44
SOR + QBO3 + HeatFlax	0.53	4.76	4.43	2.65	1.18	0.69	0.34	0.44
SOR + QBO3 + SAM	0.51	4.72	4.15	2.66	1.35	0.71	0.35	0.45
SOR + QBO3 + AOD + ENSO + HeatFlux + SAM + EqLat	**0.35**	**3.98**	**3.72**	**2.45**	**1.07**	**0.60**	**0.30**	**0.39**
Summer (JFM)								
SOR + QBO1(30 hPa)	0.59	4.39	3.28	3.39	1.91	0.85	0.35	0.46
SOR + QBO2(50 hPa)	0.59	4.39	**3.15**	3.44	1.78	0.85	0.35	0.45
SOR + QBO3(30 hPa and 50 hPa) + AOD	0.61	4.66	3.18	3.42	**1.73**	**0.72**	0.33	0.44
SOR + QBO3 + ENSO	0.58	4.27	3.51	**3.31**	**1.73**	0.78	0.35	0.46
SOR + QBO3 + EqLat	0.58	4.30	3.27	3.66	1.74	**0.72**	**0.31**	**0.41**
SOR + QBO3 + HeatFlax	0.63	4.94	3.69	3.59	1.86	0.84	0.35	0.46
SOR + QBO3 + SAM	0.62	4.89	3.72	3.59	1.83	0.84	0.35	0.46
SOR + QBO3 + AOD + ENSO + HeatFlux + SAM + EqLat	**0.52**	**4.10**	3.78	3.48	1.83	0.82	0.35	0.44
Spring (SON)								
SOR + QBO1(30 hPa)	1.06	10.79	10.61	6.60	2.93	1.31	0.51	0.67
SOR + QBO2(50 hPa)	1.09	11.10	10.82	6.64	3.11	1.39	0.52	0.68
SOR + QBO3(30 hPa and 50 hPa) + AOD	0.91	9.67	10.52	6.48	3.01	1.37	0.51	0.66
SOR + QBO3 + ENSO	1.00	10.60	10.19	6.53	3.00	1.32	0.51	0.66
SOR + QBO3 + EqLat	1.05	10.82	10.55	6.14	2.73	1.19	0.48	0.62
SOR + QBO3 + HeatFlax	0.98	10.74	10.25	5.66	2.46	1.24	0.49	0.64
SOR + QBO3 + SAM	0.89	8.62	8.62	5.01	2.55	1.18	0.47	0.60
SOR + QBO3 + AOD + ENSO + HeatFlux + SAM + EqLat	**0.78**	**8.27**	**7.85**	**4.04**	**1.49**	**0.81**	**0.32**	**0.41**

ACPD
13, 379–435, 2013

Long term changes in the upper stratospheric ozone at Syowa, Antarctica

K. Miyagawa et al.

Table 2. Continued.

(b) Optimal time-lag to the ozone for proxies (Months)								
	LAYER							
	1	2 + 3	4	5	6	7	8	8 + 9 + 10
SOR + QBO30(FUB-30 hPa)	24	24	22	18	22	8	8	8
SOR + QBO50(FUB-50 hPa)	22	1		12	14	2	4	3
SOR + QBO30 + QBO50 + AOD	10	10	6	12	14		2	2
SOR + QBO30 + QBO50 + ENSO	20		14	16	18	18	18	18
SOR + QBO30 + QBO50 + EqLat								
SOR + QBO30 + QBO50 + Heat Flux	14	4	4	2	2	14	16	16
SOR + QBO30 + QBO50 + SAM	2	2				2	2	3

ACPD
13, 379–435, 2013

Table 3. Comparison with Umkehr data and SBUV V8.6MOD OP at Umkehr Layer 8 + 9 + 10. (Annual) all seasons year, (spring) spring season (August through November), (summer) summer season (December through April). The offset ozone is UMK – SBUV V8.6MOD OP. R is correlation coefficient.

	1978–2001			2001–2011			1978–2011		
	Slope	Offset	R	Slope	Offset	R	Slope	Offset	R
V8.6MOD OP									
Annual	1.04	0.0	0.79	1.06	−0.3	0.50	1.03	−0.1	0.71
Spring	1.30	−0.5	0.77	0.90	−1.0	0.79	1.15	−0.7	0.71
Summer	0.71	+0.5	0.57	−1.03	−0.5	0.28	0.64	+0.4	0.42
V8.6MOD OP Same day									
Aug	0.68	+1.4	–	0.67	−3.2	–	1.03	−0.9	0.39
Sep	1.12	−0.6	0.84	0.49	−1.1	0.61	1.00	−0.9	0.77
Oct	1.25	−0.6	0.86	0.93	−0.8	0.93	1.12	−0.7	0.88
Nov	1.41	−0.1	0.89	1.65	0.0	0.93	1.48	−0.1	0.88
Dec	−1.52	0.0	−0.61	2.38	+0.6	0.90	−0.37	+0.6	−0.14
Jan	1.24	+0.8	0.67	−1.05	+1.0	−0.28	0.76	+0.9	0.42
Feb	0.51	+0.4	0.33	−0.13	+0.9	−0.08	0.21	+0.6	0.15
Mar	0.56	+0.1	0.40	−0.43	+0.3	−0.20	0.49	+0.2	0.31
Apr	2.85	−0.8	094	1.32	−0.7	0.73	2.34	−0.7	0.87
Annual	1.01	0.0	0.80	0.53	−0.1	0.58	1.00	0.0	0.78
Spring	1.34	−0.3	0.87	1.02	−0.8	0.80	1.33	−0.5	0.85
Summer	0.90	+0.3	0.69	0.39	+0.5	0.52	0.74	+0.4	0.64

ACPD
13, 379–435, 2013

Table 4. Calculated ozone trend from Umkehr at Syowa[a]. The linear trends are associated with EESC (polar 2) fit for 2001–2011.

Layer	1977–2001					
	Spring (% decade^{-1}, 95 % CONFI)		Summer (% decade^{-1}, 95 % CONFI)		Annual (% decade^{-1}, 95 % CONFI)	
1	−9.8	2.3	−2.0	1.7	−6.6	1.1
2 + 3	−37.0	8.7	−2.5	2.7	−16.5	3.1
4	−41.4	11.5	0.4	3.0	−15.8	3.9
5	−18.6	5.9	−0.9	4.4	−9.7	3.1
6	−7.2	2.5	−7.6	3.2	−7.4	1.7
7	−9.0	2.2	−11.3	2.3	−9.7	1.6
8	−12.1	1.7	−10.1	2.4	−10.4	1.9
8 + 9 + 10	−10.4	1.4	−8.6	2.1	−8.8	1.6
	2001–2011					
1	1.4	2.0	0.4	1.5	1.1	1.2
2 + 3	6.5	7.9	0.5	2.4	2.9	2.8
4	7.1	9.1	−0.2	2.9	2.5	3.0
5	2.9	3.9	−0.4	2.9	1.2	2.3
6	1.1	1.9	0.4	2.8	0.8	2.1
7	1.7	3.4	1.4	3.4	1.6	3.0
8	2.3	4.2	1.6	2.9	1.9	3.1
8 + 9 + 10	2.0	3.6	1.4	2.5	1.7	2.6

[a] Ozone trend and 95 % confidence (95 % CONFI) show spring (September to November), summer (January to March), and the annual. Seasonal variation, effects of solar activity, QBO, AOD, SAM, ENSO, Heat Flux and EqLat signals are removed from the data.

ACPD
13, 379–435, 2013

Long term changes in the upper stratospheric ozone at Syowa, Antarctica

K. Miyagawa et al.

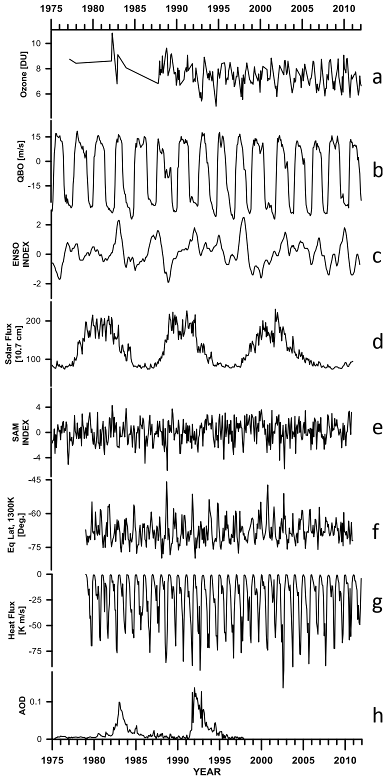

Fig. 1. Contribution of proxies to the layer-8 ozone variability Time series of monthly average variability showing **(a)** layer 8 ozone, **(b)** QBO (30 hPa), **(c)** ENSO index, **(d)** solar flax, **(e)** SAM index, **(f)** Equivalent latitude (1300 K), **(g)** Heat Flux (55–75° S average at 10-hPa) and **(h)** AOD (aerosol optical depth).

ACPD
13, 379–435, 2013

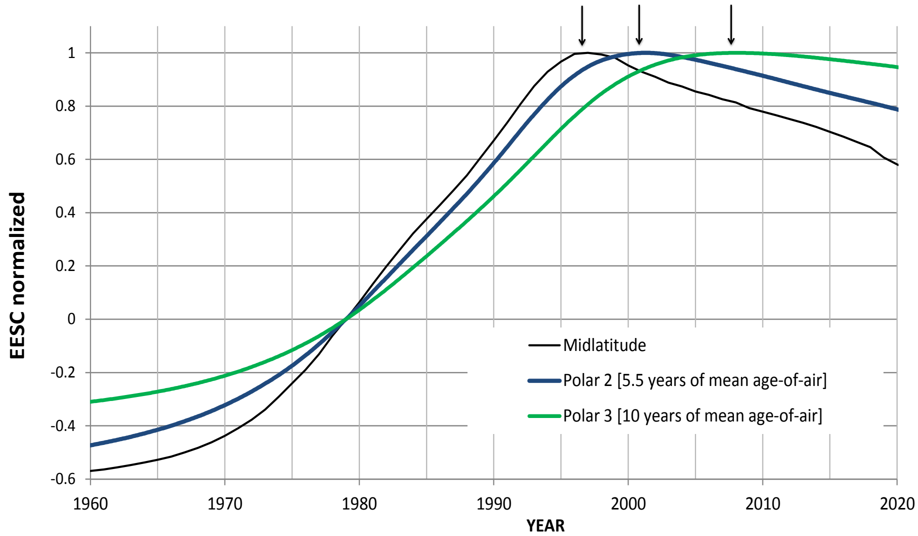

Fig. 2. EESC (Equivalent Effective Stratospheric Chlorine) curve fit associated with changes in the ODS. Mid-latitude curve shows the estimate based on 2010 WMO scenario. For polar stations, Polar-2 curve used 5.5 yr of mean age-of-air of 2010 WMO scenario. Polar-3 curve shows EESC applying an 10 yr as mean age-of-air values. The arrow indicates the peak of chlorine concentration.

ACPD
13, 379–435, 2013

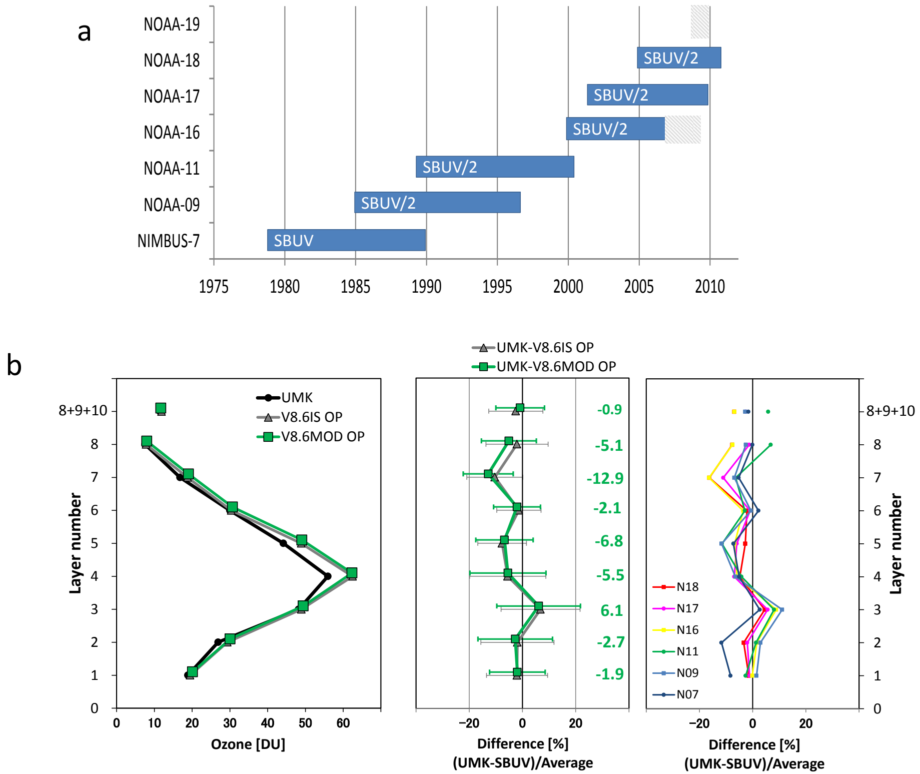

Fig. 3. SBUV(/2) satellites operational time, the vertical profile of Umkehr and overpass ozone over Syowa. **(a)** The operational time of the various NOAA satellites over Syowa are shown, with the shaded (crosshatch) sections indicating time periods for NOAA-16 or NOAA-19 operations not used in time series. **(b)** Left panel presents averaged profiles for Umkehr and SBUV, V8.6 overpass set, including individual satellites (IS) and MOD data. Middle panel shows the difference for the UMK and SBUV V8.6. The value presents UMK and SBUV ozone column difference (green square). Right panel shows the difference of UMK with SBUV V8.6 data color codes by individual satellites. The error bar is ± 1 sigma.

ACPD
13, 379–435, 2013

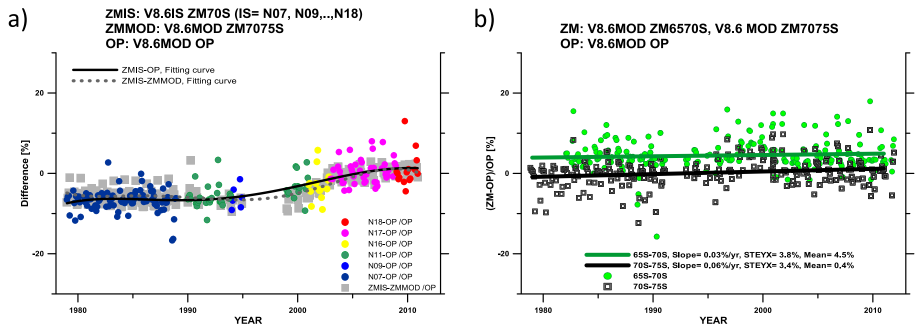

Fig. 4. Time series of the ozone rate of overpass and zonal mean derived from the SBUV V8.6 above 4 hPa. **(a)** Time series of V8.6IS ZM70S/V8.6MOD OP from individual satellites (Fitting curve is determined by a 6-degree polynomial), **(b)** Time series by two ZMs (V8.6MOD ZM6570S, V8.6MOD ZM7075S) of ZM/V8.6MOD OP.

ACPD
13, 379–435, 2013

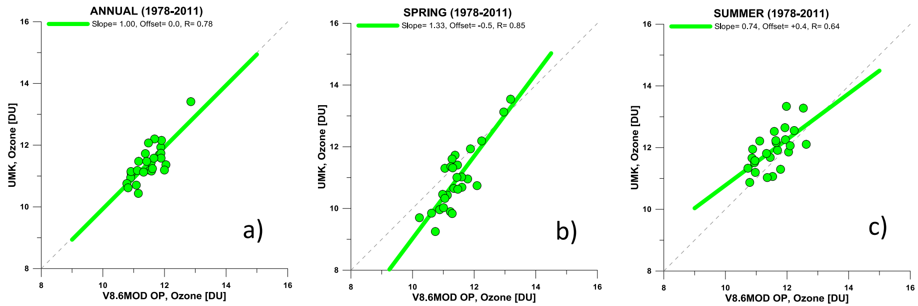

Fig. 5. Scatter plots of annual and seasonally averaged Umkehr and SBUV V8.6 MOD overpass ozone in layer 8 + 9 + 10 (above 4 hPa). Symbols represent monthly averages of the data restricted by the 24 h co-incidence criteria. The legend at the top of each plot provides information on the slope of the linear fit in the data, offset (calculated as the mean difference between UMK and SBUV OP ozone in DU), and correlation coefficient. Data comparisons are separated in three periods: **(a)** August through April (annual mean), **(b)** August through November, **(c)** December through April.

ACPD
13, 379–435, 2013

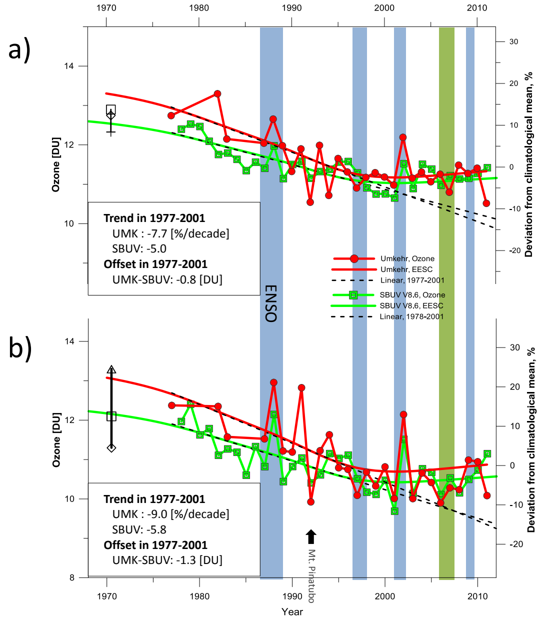

Fig. 6. Long-term variations of ozone amount in layer 8 + (above 4 hPa or 40 km altitude). Umkehr data (red circles) at Syowa and SBUV overpass data (Green squares: V8.6MOD OP), **(a)** annual mean, and **(b)** springtime three-month average (from September to November). The red and green lines show the EESC (Polar 2) fit in Umkehr and SBUV data respectively. The dashed lines show linear ozone trends derived from 1977 (1978)–2001 period. The annual cycle, effects of solar activity and QBO (50 hPa) signals were removed from the data prior to the ozone record trend analysis. The blue shade indicates the period of El Nino and the yellow-green shade indicates the period of La Nina. Three symbols on the left side of the plot represent 1957-1972 averaged ozone from 3 stations, Faraday (65° S), King Baudouin (70° S), and Halley (73.5° S).

ACPD
13, 379–435, 2013

Long term changes in the upper stratospheric ozone at Syowa, Antarctica

K. Miyagawa et al.

Title Page
Abstract | Introduction
Conclusions | References
Tables | Figures
◀| |▶
◀ ▶
Back | Close
Full Screen / Esc
Printer-friendly Version
Interactive Discussion

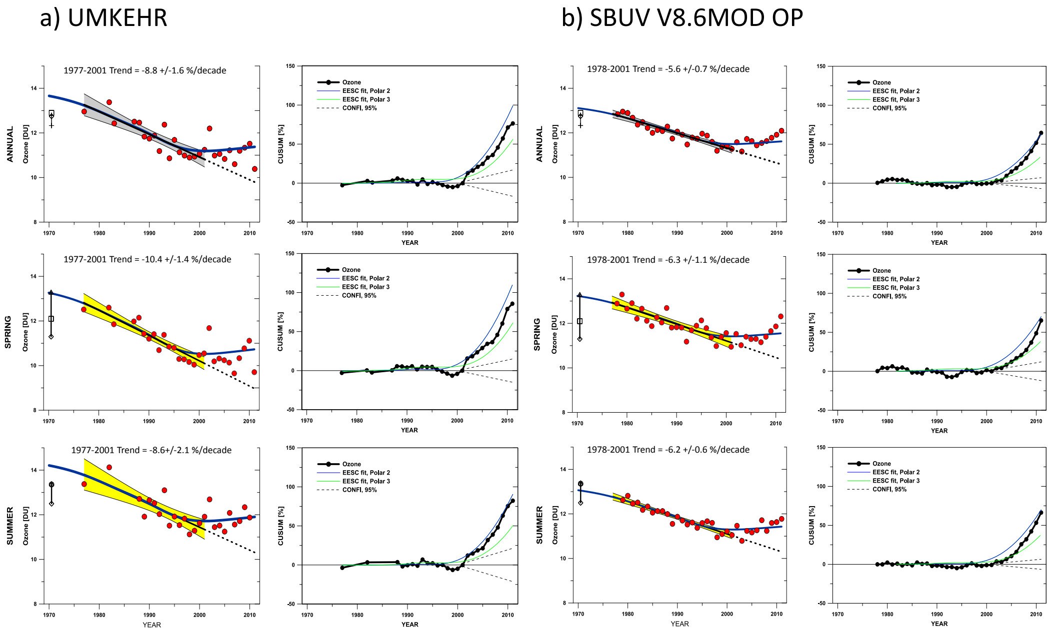

Fig. 7. Time series of monthly ozone variability (red circles) in layer 8+ **(a)** and layer 4 **(c)** in the Antarctic Syowa (69° S); (right) cumulative sum (CUSUM) in percent. Similarly, **(b)** and **(d)** show time series change of SBUV V8.6MOD OP over the Syowa. Upper panels are annual mean (from January to March, and August to December), and middle panels show the three-month average for springtime (from September to November) and bottom panels summertime (from January to March). Ozone trend is derived after removing ozone variability explained by effects such as the seasonal variation, solar activity, QBO, AOD, EqLat, SAM, Heat Flux and ENSO signals. The dotted line is the ozone trend calculated from the observation for 1977 to 2001, and indicates the trend forecast afterward linearly, and 95 % of confidence level envelope is shown. (left) the Y-axis of Spring and Summer adjusts a seasonal mean value. The blue line shows the EESC curve (Polar 2) representative of effective stratospheric chlorine load at high latitude, and thick broken lines show linear trends from 1977 to 2001. Shaded area indicates 95 % confidence intervals. Three symbols on the left side of the plot represent 1957–1972 averaged ozone from 3 stations, Faraday (65° S), King Baudouin (70° S), and Halley (73.5° S). (right) Blue and the green line show cumulative sum for EESC Polar region. The dotted line indicate the 95 % confidence envelopes of departure from natural variability and model uncertainty.

ACPD
13, 379–435, 2013

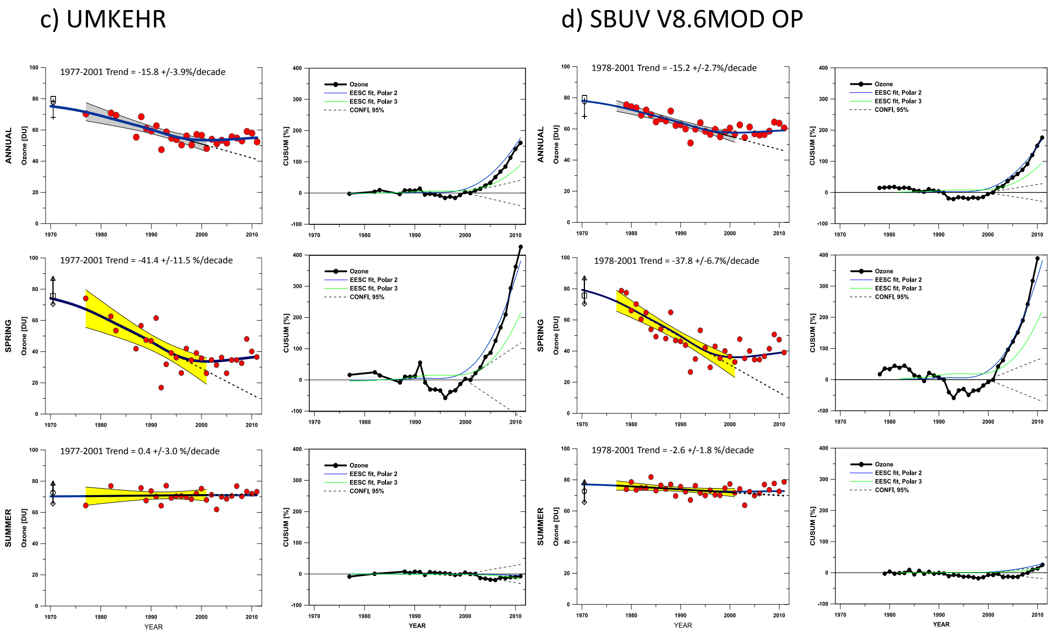

Fig. 7. Continued.

Discussion Paper | Discussion Paper | Discussion Paper | Discussion Paper |

ACPD

13, 379–435, 2013

Long term changes in the upper stratospheric ozone at Syowa, Antarctica

K. Miyagawa et al.

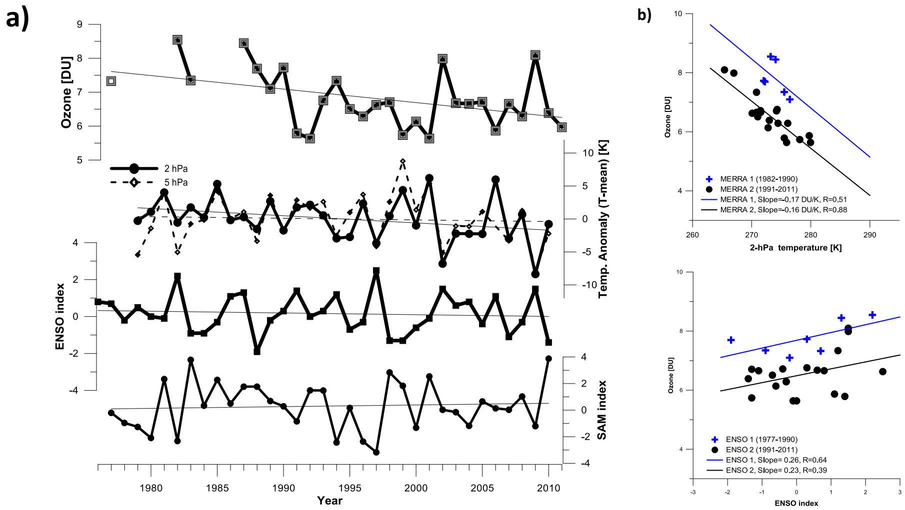

Fig. 8. Layer 8 Ozone time series compared to SAM, Temperature and ENSO. Ozone, Temperature, and ENSO are November averages. SAM is October to December Average. **(a)** Time series layer-8 ozone, temperature anomaly at 2-hPa and 5-hPa pressure levels from MERRA data, SAM index are September–November mean ENSO index. Layer-8 ozone are shown after subtraction of seasonal, solar activity, and QBO related variability. **(b)** The scatter diagram in each ten years of the MERRA temperature (upper), and preceded scatter diagram for ENSO (bottom).

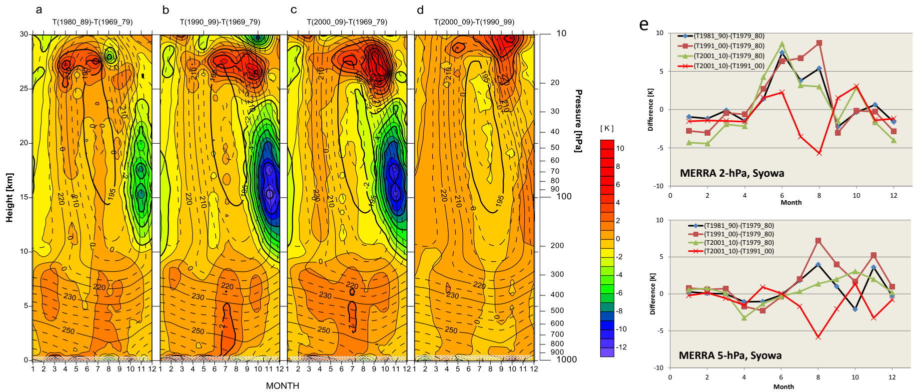

Fig. 9. Decadal temperatures changes over Syowa based on measurements by radiosondes. **(a–c)** show the changes from pre-ozone hole period averages (1969–1979) for the 1980s, 1990s and 2000s. **(d)** shows the change from 1990s to 2000s. The color level shows a temperature difference and the contour lines the 10-year average temperature. The radiosonde record has had four changes of instruments (from 1969 using RSII-69, from 1980 using RS2-78, from 1987 using RS2-80 and from 1995 using RSII-91). Decadal changes in the same ranges using MERRA data at two levels are displayed in **(e)**.

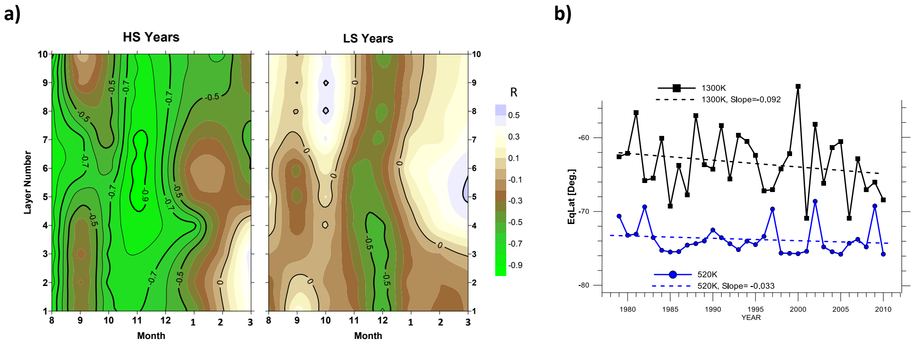

Fig. 10. (a) Plots show correlation (R) between ozone and the mean Southern Annular Mode (SAM) index as function of altitude (Umkehr layers) and month. Correlation between SAM-index and the ozone is sought for high (HS) and low (LS) periods in the solar cycle (maximum and minimum of the Solar cycle respectively). **(b)** Time series of the difference between equivalent latitude and Syowa station latitude (−69°) are plotted for the three-month mean (September–October–November). The Equivalent latitude is derived from MERRA analysis at 1300 K or 3 hPa and at 520 K or 50 hPa.

ACPD
13, 379–435, 2013

ACPD
13, 379–435, 2013

Long term changes in the upper stratospheric ozone at Syowa, Antarctica

K. Miyagawa et al.

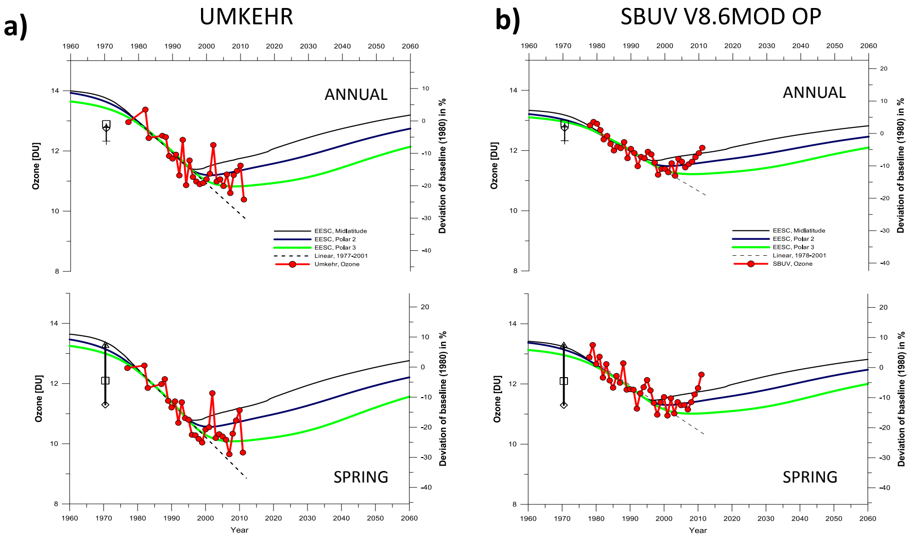

Fig. 11. Long-term variations of ozone amount in layer 8+9+10 (above 4 hPa or 40 km altitude). Umkehr data **(a)** at Syowa and SBUV V8.6MOD overpass data **(b)**. Similar to Fig. 6, with ozone residuals derived from the full statistical model that includes additional explanatory parameters, such as AOD, EqLat, SAM, Heat Flux and ENSO signals. Here, upper panel shows results for annual mean (from January to March, and August to December), and bottom panel show the three-month average for springtime (from September to November). The same data are used in the top two panels shown on the left side of Fig. 7a. The dotted line is the ozone trend calculated from the observation taken from 1977 until 2001, whereas after 2001 it indicates the scenario for continuous ozone depletion in the absence of the Montreal protocol. Three EESC curves represent several scenarios for the Montreal protocol related changes in ODS concentrations in the upper stratosphere at the middle (black) and high latitudes (two curves, blue and green). These curves show similar linear trends during ozone depletion in 1977–2001 time period.